3rd Workshop on Density Functional Theory (DFT2025):
Fundamentals, Developments, and Applications
RIKEN Kobe Campus
2025.3.25-27(26)

Time Dependent Density Functional Theory for Extremely Nonlinear Optics

Kazuhiro Yabana

**Center for Computational Sciences,
University of Tsukuba**

Today I will talk on:

- **Solve Maxwell and Schrödinger (time-dependent Kohn-Sham) equations simultaneously.**
- **Directly connecting electromagnetism and quantum mechanics.**

Classical electromagnetic fields

$$\nabla \times \nabla \times \mathbf{A} + \frac{1}{c^2}\frac{\partial^2}{\partial t^2}\mathbf{A} = \frac{4\pi}{c}\mathbf{j}$$

Quantum electronic motion

$$i\hbar\frac{\partial}{\partial t}\psi_i = \left\{ \frac{1}{2m}\left(-i\hbar\nabla + \frac{e}{c}\mathbf{A}\right)^2 + V_{ion} + V_H + V_{xc} \right\}\psi_i$$

$$\mathbf{j} = -\frac{e}{2m}\left\{ \psi_i^* \left(-i\hbar\nabla + \frac{e}{c}\mathbf{A}\right)\psi_i + c.c. \right\}$$

- **Why and where it is necessary?** ⟹ **Extreme Optics**
- **How it is carried out?**
- **How it works?**

Light-matter interaction:
usually characterized by dielectric function/index of refraction

$$n = \sqrt{\varepsilon}$$

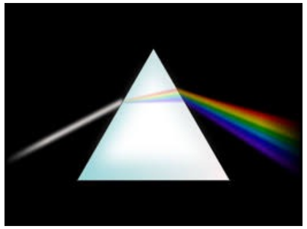

Dispersion (freq. dep.) $n(\omega), \quad \varepsilon(\omega)$

Nonlinearity (Intensity dep.) $n = n_0 + n_2 E^2$

Transparent dielectric
= real dielectric function/index of refraction
for visible frequencies (~1.5-3.0 eV)

Dielectric function of diamond

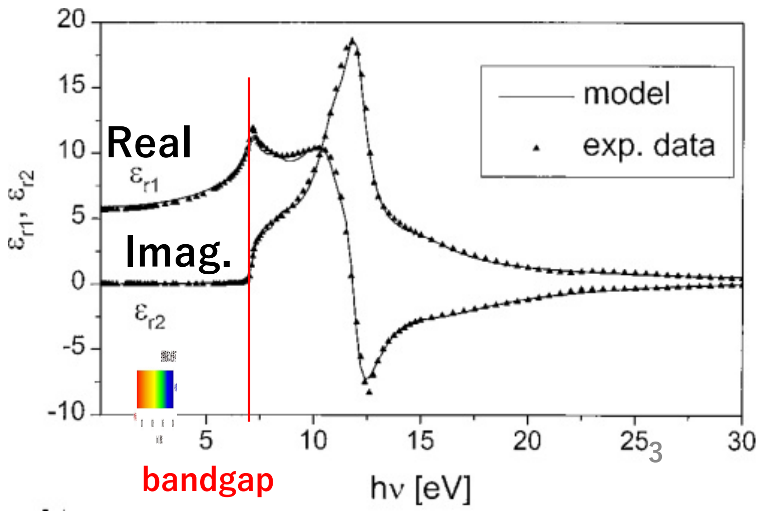

Dielectric function is not complete/sufficient for optics!

Glass becomes absorptive for very strong light: Laser processing

$\mathrm{Im}\,\varepsilon = 0$ ⟹ $\mathrm{Im}\,\varepsilon \neq 0$ **Nonlinearity**

Transparent **Absorptive**

Such process cannot be described within ordinary electromagnetism.

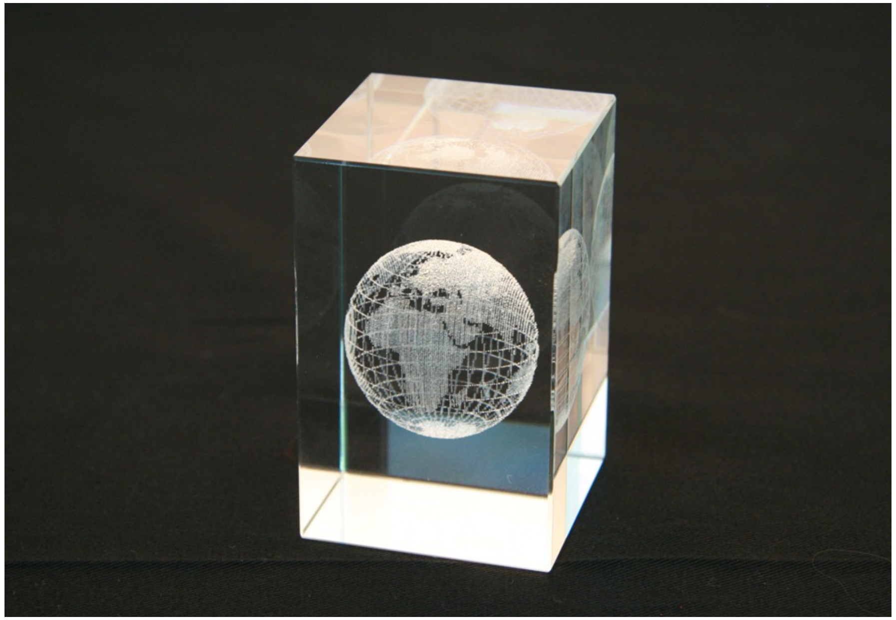

Optics: Two aspects of light-Matter interaction

Light propagation (Maxwell's)eq.

$$\nabla \cdot \boldsymbol{B} = 0$$
$$\nabla \times \boldsymbol{E} + \frac{\partial \boldsymbol{B}}{\partial t} = \boldsymbol{0}$$
$$\nabla \cdot \boldsymbol{D} = \rho$$
$$\nabla \times \boldsymbol{H} - \frac{\partial \boldsymbol{D}}{\partial t} = \boldsymbol{j}$$

e.g, FDTD (Finite-difference
time-domain method)

First-principles quantum mechanics calculations of optical constants

$$\varepsilon_r = 1 + \frac{2Ne^2}{\varepsilon_0 \hbar} \sum_j \frac{\omega_{j0} \left| \langle 0 | x | j \rangle \right|^2}{\omega_{j0}^2 - (\omega + i\gamma)^2}$$

e.g, GW-BS, TDDFT

Constitutive relation

$$\boldsymbol{D}(\boldsymbol{r}, \boldsymbol{t}) = \int_{-\infty}^{t} \boldsymbol{dt'} \boldsymbol{\epsilon}(\boldsymbol{t} - \boldsymbol{t'}) \boldsymbol{E}(\boldsymbol{r}, \boldsymbol{t'})$$

$$\boldsymbol{D}(\boldsymbol{r}, \boldsymbol{\omega}) = \boldsymbol{\epsilon}(\boldsymbol{\omega}) \boldsymbol{E}(\boldsymbol{r}, \boldsymbol{\omega})$$

Electromagnetism (EM)

Quantum Mechanics (QM)

- **EM and QM are separated using constitutive relation.**
- **Usually, linear and local constitutive relation is assumed.**

$$\mathbf{D} = \mathbf{E} + 4\pi \mathbf{P} \qquad \mathbf{P}(\mathbf{r}, t) = \int^{t} dt' \chi(t - t') \mathbf{E}(\mathbf{r}, t')$$

Extreme Optics

In frontiers of optical science using extreme pulsed light

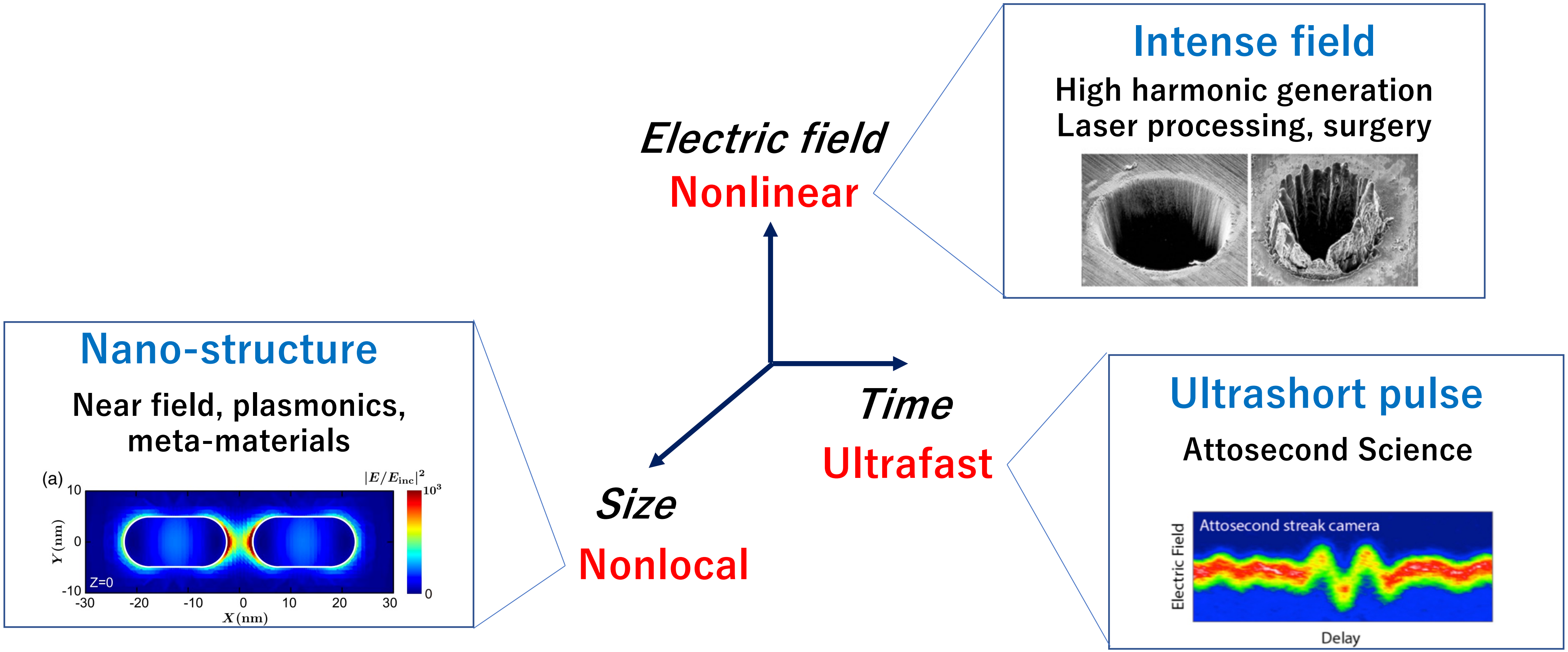

Recent Nobel prizes in related fields

Strong Light: Nonlinearity

The Nobel Prize in Physics 2018

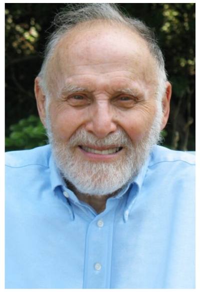

© Arthur Ashkin
Arthur Ashkin
Prize share: 1/2

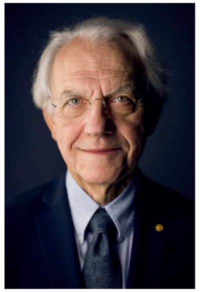

© Nobel Media AB. Photo: A. Mahmoud
Gérard Mourou
Prize share: 1/4

© Nobel Media AB. Photo: A. Mahmoud
Donna Strickland
Prize share: 1/4

"For their method of generating **high-intensity, ultra-short optical pulses**" (Mourou, Strickland)

Short-pulse: Ultrafast

The Nobel Prize in Physics 2023

Ill. Niklas Elmehed © Nobel Prize Outreach
Pierre Agostini
Prize share: 1/3

Ill. Niklas Elmehed © Nobel Prize Outreach
Ferenc Krausz
Prize share: 1/3

Ill. Niklas Elmehed © Nobel Prize Outreach
Anne L'Huillier
Prize share: 1/3

"For experimental methods that generate **attosecond pulses of light** for the study of **electron dynamics in matter**"

Nano: Nonlocality

The Nobel Prize in Chemistry 2023

Ill. Niklas Elmehed © Nobel Prize Outreach
Moungi G. Bawendi
Prize share: 1/3

Ill. Niklas Elmehed © Nobel Prize Outreach
Louis E. Brus
Prize share: 1/3

Ill. Niklas Elmehed © Nobel Prize Outreach
Aleksey Yekimov
Prize share: 1/3

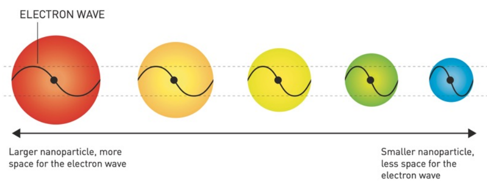

They planted an important seed for nanotechnology

https://www.nobelprize.org/prizes/

Nonlinearity: strong laser pulse on materials

High harmonic generation from solids

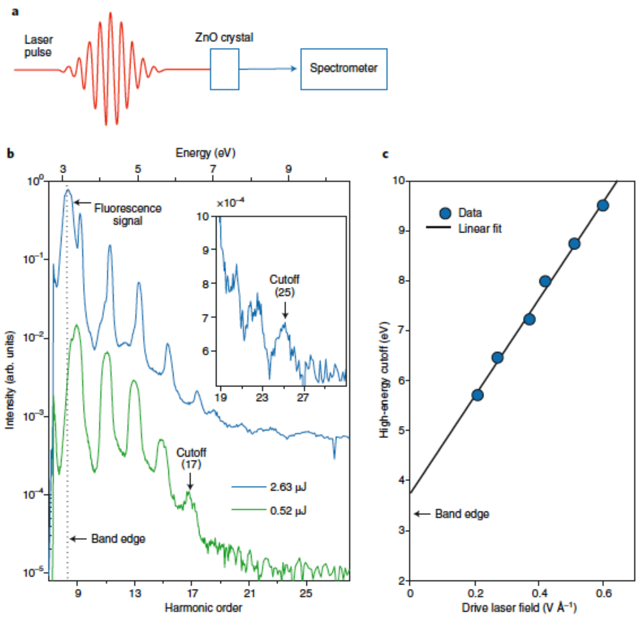

S. Ghimire et al, Nat. Phys. 7, 138 (2011)
S. Ghimire, D.A. Reis, Nature Physics 15, 10 (2019)

$$P(\mathbf{r},t) = \int dt' \chi^{(1)}(t-t')E(\mathbf{r},t')$$

$$P(\mathbf{r},t) = \int dt' \chi^{(1)}(t-t')E(\mathbf{r},t') + \int dt'dt'' \chi^{(2)}(t-t',t-t'')E(\mathbf{r},t')E(\mathbf{r},t'')$$
$$+ \int dt'dt''dt''' \chi^{(3)}(t-t',t-t'',t-t''')E(\mathbf{r},t')E(\mathbf{r},t'')E(\mathbf{r},t''') + \cdots$$

Spatially local, but highly nonlinear

Explicit construction of nonlinear susceptibilities is difficult and useless.

Nonlocality: optical response in nano-material

Quantum Tunneling in Plasmonics

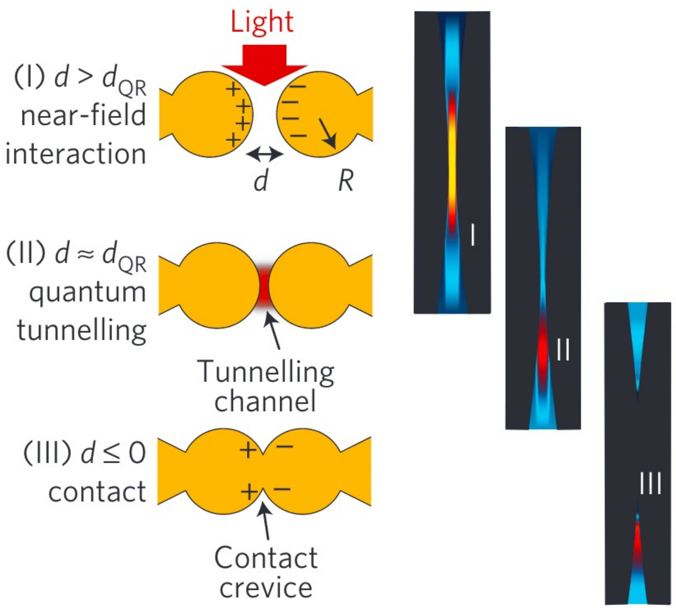

M.S. Tame et.al, Nature Phys. 9, 329 (2013)

$$P(\mathbf{r}, t) = \int dt' \chi^{(1)}(t - t') E(\mathbf{r}, t')$$

$$P(\mathbf{r}, t) = \int dt' \int d\mathbf{r}' \chi^{(1)}(\mathbf{r}, \mathbf{r}', t - t') E(\mathbf{r}', t')$$

Linear, but spatially nonlocal

Explicit construction of nonlocal susceptibility is difficult and useless.

Today I will talk on:

- **Solve Maxwell and Schrödinger (time-dependent Kohn-Sham) equations simultaneously.**
- **Directly connecting electromagnetism and quantum mechanics.**

Classical electromagnetic fields

$$\nabla \times \nabla \times \mathbf{A} + \frac{1}{c^2}\frac{\partial^2}{\partial t^2}\mathbf{A} = \frac{4\pi}{c}\mathbf{j}$$

Quantum electronic motion

$$i\hbar\frac{\partial}{\partial t}\psi_i = \left\{ \frac{1}{2m}\left(-i\hbar\nabla + \frac{e}{c}\mathbf{A}\right)^2 + V_{ion} + V_H + V_{xc} \right\}\psi_i$$

$$\mathbf{j} = -\frac{e}{2m}\left\{ \psi_i^* \left(-i\hbar\nabla + \frac{e}{c}\mathbf{A}\right)\psi_i + c.c. \right\}$$

- **Why and where it is necessary?**
- **How it is carried out?**
- **How it works?**

Classical electromagnetic fields

$$\nabla \times \nabla \times \mathbf{A} + \frac{1}{c^2}\frac{\partial^2}{\partial t^2}\mathbf{A} = \frac{4\pi}{c}\mathbf{j}$$

Quantum electronic motion

$$i\hbar\frac{\partial}{\partial t}\psi_i = \left\{\frac{1}{2m}\left(-i\hbar\nabla + \frac{e}{c}\mathbf{A}\right)^2 + V_{ion} + V_H + V_{xc}\right\}\psi_i$$

$$\mathbf{j} = -\frac{e}{2m}\left\{\psi_i^*\left(-i\hbar\nabla + \frac{e}{c}\mathbf{A}\right)\psi_i + c.c.\right\}$$

We first consider description of electronic motion for a given electric field, E(t).

Atoms irradiated by strong pulsed electric field

Electron rescattering and high harmonic generation by TDDFT

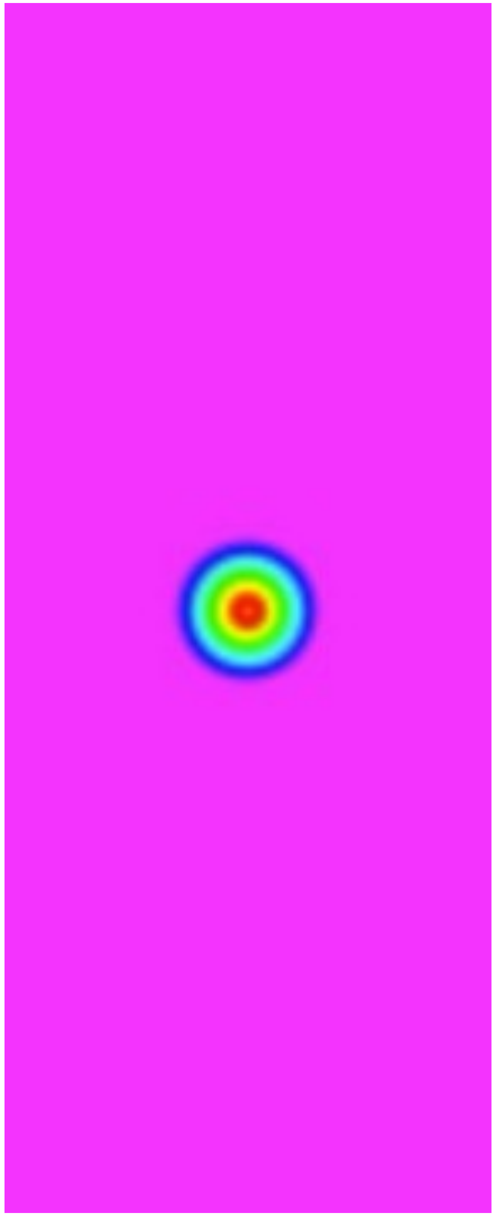

Applied laser field

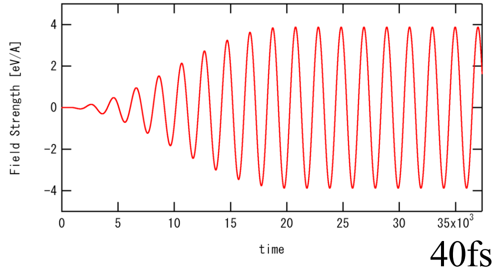

40fs

$$\frac{dD(t)}{dt} = \frac{d}{dt}\int d\vec{r}\, z\rho(\vec{r},t)$$

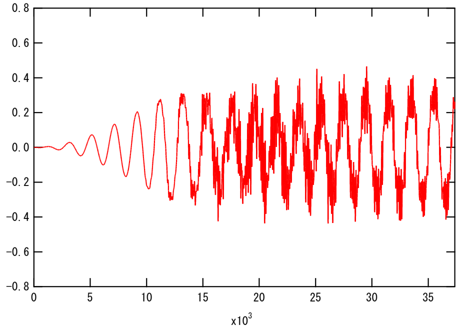

$$I(\omega) \propto \left| \int dt e^{i\omega t} d_A(t) \right|^2$$

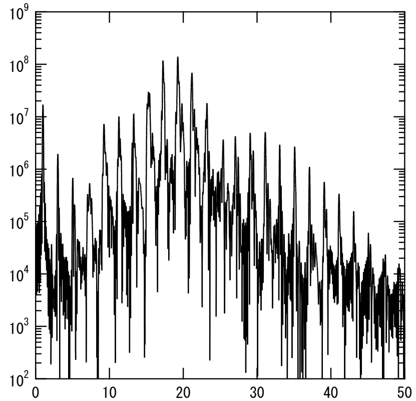

harmonic order (frequency)

Ar atom
2×10^{14}W/cm^2
800nm
TDDFT(ALDA)

Time-dependent Kohn-Sham equation

$$i\hbar\frac{\partial}{\partial t}\psi_i(\mathbf{r},t) = \left\{-\frac{\hbar^2}{2m}\nabla^2 + V_{\text{ion}}(\mathbf{r}) + \int d\mathbf{r}'\frac{e^2}{|\mathbf{r}-\mathbf{r}'|}\rho(\mathbf{r}',t) + \mu_{xc}(\mathbf{r},t) + V_{\text{ext}}(\mathbf{r},t)\right\}\psi_i(\mathbf{r},t)$$

$$\rho(\mathbf{r},t) = \sum_i |\psi_i(\mathbf{r},t)|^2 \qquad V_{\text{ext}}(\mathbf{r},t) = e\mathbf{E}(t)\cdot\mathbf{r}$$

Numerical method adopted throughout my presentation

Real-space uniform grid

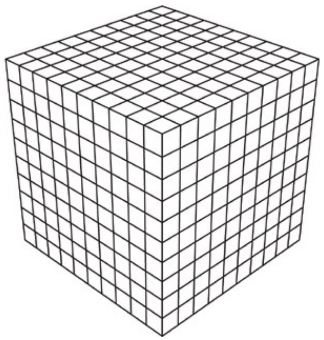

Norm-conserving pseudopotential

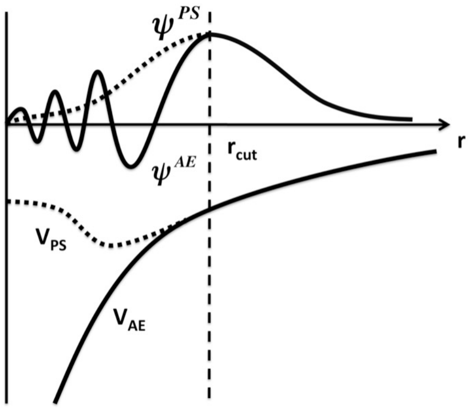

High order finite difference (9pts) for spatial derivative

Explicit method for time evolution

$$\psi(t+\Delta t) = e^{iH\Delta t/\hbar}\psi(t) \approx \sum_{k=0}^{N}\left(\frac{1}{k!}\frac{i\Delta t H}{\hbar}\right)^k \psi(t)$$

Crystalline solids irradiated by strong pulsed electric field

The potential $eE(t)x$ is called "length gauge".

In this "length gauge", lattice periodicity is violated so that Bloch theorem cannot be applied.

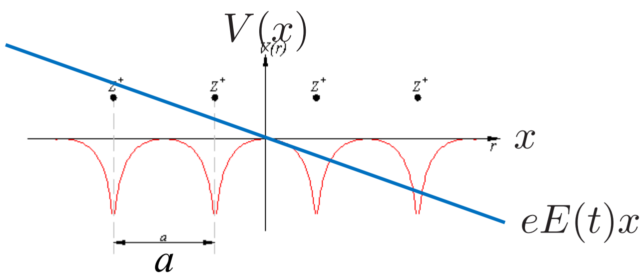

$$V(x+a) \neq V(x)$$

We will make use of gauge freedom to overcome the problem.

Gauge transformation: from "length gauge" to "velocity gauge"

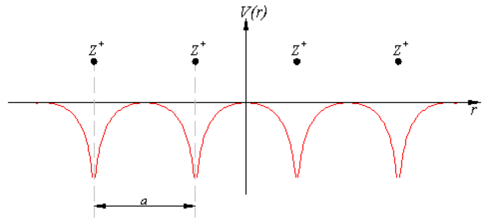

Length gauge

$$i\hbar\frac{\partial}{\partial t}\psi = \left\{\frac{1}{2m}\left(-i\hbar\vec{\nabla}\right)^2 + V(\vec{r}) + \underline{e\vec{E}(t)\cdot\vec{r}}\right\}\psi$$

$$\psi' = \exp\left[\frac{ie}{\hbar c}\vec{A}(t)\cdot\vec{r}\right]\psi$$

$$\vec{E}(t) = -\frac{1}{c}\frac{d\vec{A}(t)}{dt}$$

Gauge transformation
using time-dependent,
spatially-uniform vector potential

Velocity gauge

$$i\hbar\frac{\partial}{\partial t}\psi' = \left\{\frac{1}{2m}\left(-i\hbar\vec{\nabla} + \underline{\frac{e}{c}\vec{A}(t)}\right)^2 + V(\vec{r})\right\}\psi'$$

**Expressing uniform electric field by vector potential,
lattice periodicity of Hamiltonian is recovered.**

$$h(\vec{r}+\vec{a}) = h(\vec{r})$$

Time-Dependent Kohn-Sham equation in velocity gauge

$$i\hbar\frac{\partial}{\partial t}\psi_i(\vec{r},t) = \left\{\frac{1}{2m}\left(-i\hbar\vec{\nabla} + \frac{e}{c}\vec{A}(t)\right)^2 - \sum_a \frac{Z_a e^2}{|\vec{r}-\vec{R}_a|} + \int d\vec{r}'\frac{e^2}{|\vec{r}-\vec{r}'|}\rho(\vec{r}',t) + \mu_{xc}[\rho(\vec{r},t)]\right\}\psi_i(\vec{r},t)$$

$$\rho(\vec{r},t) = \sum_i |\psi_i(\vec{r},t)|^2$$

At each time, we may apply the Bloch's theorem

$$\psi_i(\vec{r},t) = e^{i\vec{k}\vec{r}}u_{n\vec{k}}(\vec{r},t)$$

$$i\hbar\frac{\partial}{\partial t}u_{n\vec{k}}(\vec{r},t) = \left\{\frac{1}{2m}\left(-i\hbar\vec{\nabla} + \hbar\vec{k} + \frac{e}{c}\vec{A}(t)\right)^2 - \sum_a \frac{Z_a e^2}{|\vec{r}-\vec{R}_a|} + \int d\vec{r}'\frac{e^2}{|\vec{r}-\vec{r}'|}\rho(\vec{r}',t) + \mu_{xc}[\rho(\vec{r},t)]\right\}u_{n\vec{k}}(\vec{r},t$$

$$u_{n\vec{k}}(\vec{r}+\vec{a},t) = u_{n\vec{k}}(\vec{r},t)$$

Further gauge transformation is possible in Bloch's space

Original length gauge $$i\hbar\frac{\partial}{\partial t}\psi = \left\{\frac{1}{2m}\left(-i\hbar\vec{\nabla}\right)^2 + V(\vec{r}) + e\vec{E}(t)\cdot\vec{r}\right\}\psi$$

$$\psi' = \exp\left[\frac{ie}{\hbar c}\vec{A}(t)\cdot\vec{r}\right]\psi$$

Velocity gauge $$i\hbar\frac{\partial}{\partial t}\psi' = \left\{\frac{1}{2m}\left(-i\hbar\vec{\nabla} + \frac{e}{c}\vec{A}(t)\right)^2 + V(\vec{r})\right\}\psi' \qquad \vec{E}(t) = -\frac{1}{c}\frac{d\vec{A}(t)}{dt}$$

Time-dependent Bloch (Kohn-Sham) equation

$$i\hbar\frac{\partial}{\partial t}u_{n\vec{k}} = \left\{\frac{1}{2m}\left(-i\hbar\vec{\nabla} + \hbar\vec{k} + \frac{e}{c}\vec{A}(t)\right)^2 + V(\vec{r})\right\}u_{n\vec{k}}$$

$$u'_{n\vec{k}}(\vec{r},t) = \exp\left[-\frac{e}{\hbar c}\vec{A}(t)\vec{\nabla}_k\right]u_{n\vec{k}}(\vec{r},t)$$

Length-gauge in k-space $$i\hbar\frac{\partial}{\partial t}u'_{n\vec{k}} = \left\{\frac{1}{2m}\left(-i\hbar\vec{\nabla} + \hbar\vec{k}\right)^2 + V(\vec{r}) + ie\vec{E}(t)\vec{\nabla}_k\right\}u'_{n\vec{k}}$$

$e\vec{E}(t)\cdot\vec{r}$

Length operator in k-space $\vec{r} \to i\nabla_k$

Dynamical Berry phase theory

C. Attaccalite, M. Grüning, Phys. Rev. B88, 235113 (2013)

I. Souza, J. Iniguez, D. Vanderbilt, Phys. Rev. 69, 085106 (2004)

Real-time TDDFT in a unit cell of silicon under strong laser pulse

Static DFT: Band calculation

$$\varepsilon_{nk} u_{nk}(r) = \left[\frac{1}{2m}(p + \hbar k)^2 + V_H(r) + V_{xc}(r)\right] u_{nk}(r)$$

TDDFT: Electron dynamics

$$i\hbar \frac{\partial}{\partial t} u_{nk}(r,t) = \left[\frac{1}{2m}\left(p + \hbar k + \frac{e}{c}A(t)\right)^2 + V_H(r,t) + V_{xc}(r,t)\right] u_{nk}(r,t)$$

$$A(t) = -c \int^t E(t')\mathrm{d}t'$$

$$\mathbf{j} = -\frac{e}{2m}\left\{\psi_i^* \left(-i\hbar\nabla + \frac{e}{c}\mathbf{A}\right)\psi_i + c.c.\right\}$$

$$E(t) = E_0 \cos^2\left(\frac{\pi t}{T}\right)\cos\omega t$$

$E_0 = 2.0$ [V/Å]

$\hbar\omega = 1.55$[eV]

$T = 20$[fs]

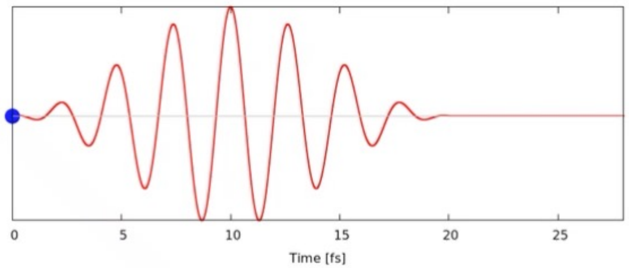

$n(\boldsymbol{r}, t)$

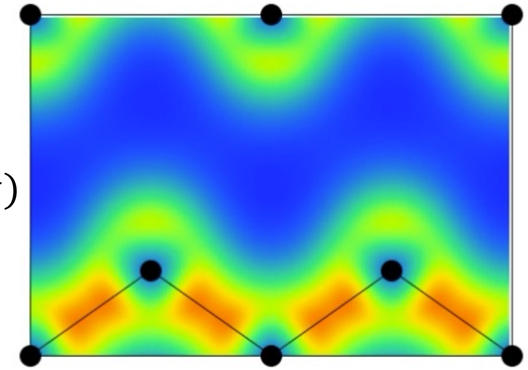

$n(\boldsymbol{r}, t) - n_{GS}(\boldsymbol{r}, t)$

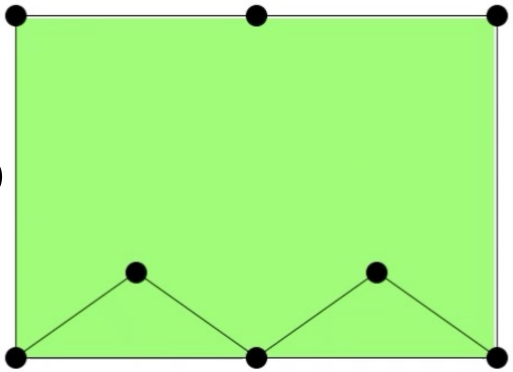

G.F. Bertsch, J.-I. Iwata, A. Rubio, K. Yabana, Phys. Rev. B62, 7998 (2000)

T. Otobe, M. Yamagiwa, J.-I. Iwata, K. Yabana, T. Nakatsukasa, K. Yabana, Phys. Rev. B77, 165104 (2008)

Real-time TDDFT in a unit cell of silicon under strong laser pulse

Electric field

$$E(t) = E_0 \cos^2\left(\frac{\pi t}{T}\right) \cos \omega t$$

$$E_0 = 2.0\ [\mathrm{V/Å}]$$
$$\hbar\omega = 1.55[\mathrm{eV}]$$
$$T = 20[\mathrm{fs}]$$

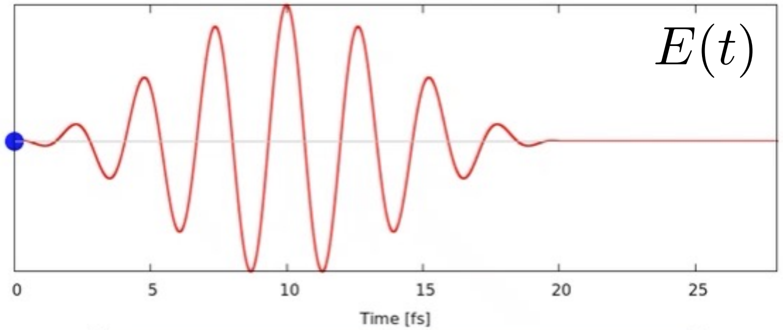

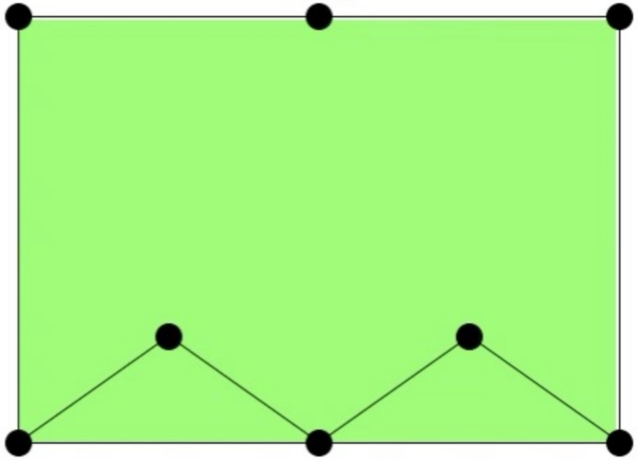

$$\Delta\rho(\mathbf{r},t) = \rho(\mathbf{r},t) - \rho_0(\mathbf{r})$$

Current density

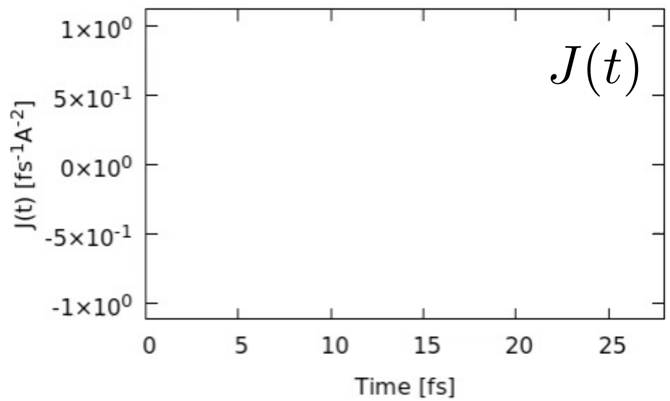

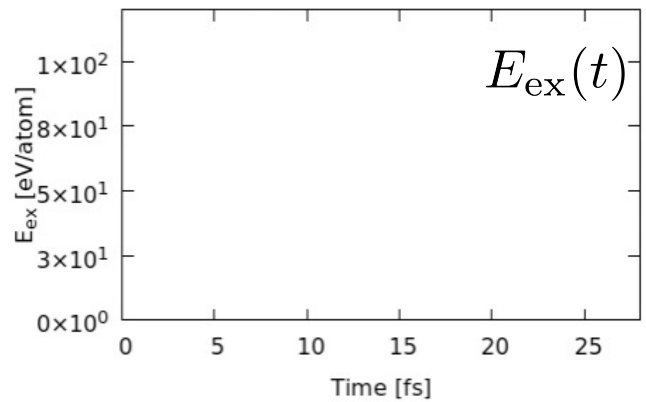

Electronic excitation energy

Real time calculation of dielectric function

G.F. Bertsch, J.-I. Iwata, A. Rubio, K. Yabana, Phys. Rev. B62, 7998 (2000)
K. Yabana, T. Sugiyama, Y. Shinohara, T. Otobe, G.F. Bertsch, Phys. Rev. B85, 045134 (2012)

Applied electric field and induced current

$$J(t) = \int^{t} dt' \underline{\sigma(t-t')} E(t')$$

Electric conductivity

$$\epsilon(\omega) = 1 + 4\pi\chi(\omega) = 1 + \frac{4\pi i \sigma(\omega)}{\omega}$$

Apply impulsive force to all electrons in the crystal

$$F_{ext}(t) = -eE(t) = I\delta(t) \qquad A(t) = -c\int^{t} dt' E(t') = A_0\theta(t) \qquad A_0 = \frac{c}{e}I$$

$$\boxed{v_{n\mathbf{k}}(\mathbf{r}, t=0_+) = u_{n\mathbf{k}+\frac{e\mathbf{A}_0}{\hbar c}}(\mathbf{r})}$$

Impulse = shift of crystal momentum, *k*

Induced current is proportional to conductivity in time domain

$$J(t) = \int dt' \sigma(t-t') E(t') = \frac{I}{-e}\sigma(t)$$

Real-time calculation of dielectric function of silicon（TDDFT-ALDA）

Current as a function of time after impulse

$$E(t) = k\delta(t) \qquad A(t) = -kc\theta(t)$$

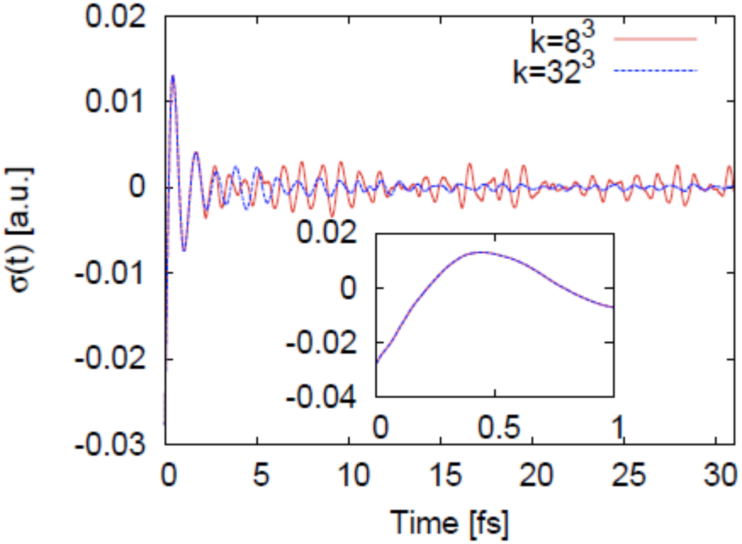

Dielectric function

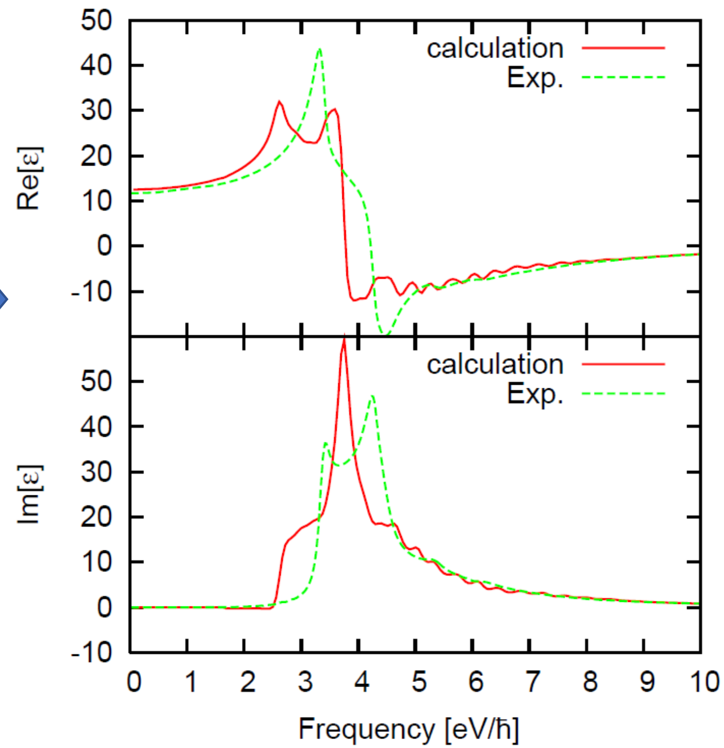

Quality not sufficient by ALDA

For the first-principles calculation of dielectric function,
"GW + Bethe-Salpeter" is the state-of-the-art.

Efforts to improve "exchange-correlation potential" in TDDFT
have continued for many years.

Improvement through A_xc(t) is considered to be important

$$i\hbar\frac{\partial}{\partial t}u_{n\mathbf{k}}(\mathbf{r},t)=\left\{-\frac{1}{2m}\left(-i\hbar\nabla+\hbar\mathbf{k}+\frac{e}{c}\mathbf{A}(t)\right)^2+V_{\rm ion}(\mathbf{r})+V_{\rm H}(\mathbf{r},t)+V_{\rm xc}(\mathbf{r},t)\right\}u_{n\mathbf{k}}(\mathbf{r},t)$$

$$\mathbf{A}_{ext}(t)+\mathbf{A}_{xc}(t)$$

Necessary for extended systems

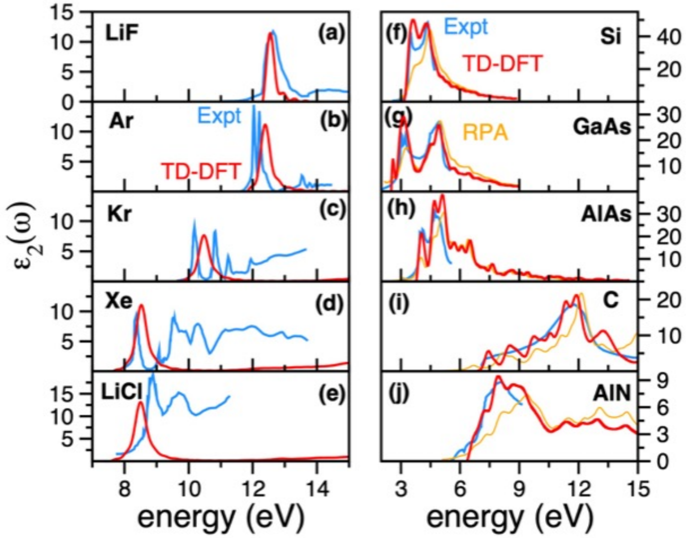

$$a_2\frac{\partial^2}{\partial t^2}\mathbf{A}_{\rm xc}(t)+a_0\mathbf{A}_{\rm xc}(t)=\frac{4\pi c}{\Omega}\mathbf{J}(t).$$

J.K. Dewhurst, D. Gill, S. Shallcross, S. Sharma,
Phys. Rev. B111, L060302 (2025)

When connecting Maxwell/Schrödinger necessary?
= when incident pulse is modulated by matter?

Not necessary

Atoms

Molecules

Small nanoparticles
(< a few nm radius)

Marginal

Monoatomic layer
(e.g. Graphene)

Single layer of graphene
absorbs 2.3% of incident light

- Single layer: not necessary
- Ten layers: necessary

Necessary

films
(> a few tens nm thick)

Nanoparticles
(> a few tens nm radius)

Bulk surfaces

Wavelength of visible light
~ 1 μm (1000 nm)

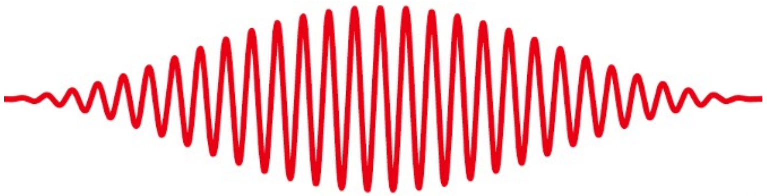

Directly connect EM and QM

Light propagation solving classical Maxwell's equations

$$\nabla \times \nabla \times \mathbf{A} + \frac{1}{c^2}\frac{\partial^2}{\partial t^2}\mathbf{A} = \frac{4\pi}{c}\mathbf{j}$$

Electron dynamics by TDDFT in real time

$$i\hbar\frac{\partial}{\partial t}\psi_i = \left\{\frac{1}{2m}\left(-i\hbar\nabla + \frac{e}{c}\mathbf{A}\right)^2 + V_{ion} + V_H + V_{xc}\right\}\psi_i$$

$$\mathbf{j} = -\frac{e}{2m}\left\{\psi_i^*\left(-i\hbar\nabla + \frac{e}{c}\mathbf{A}\right)\psi_i + c.c.\right\}$$

We develop two methods, without/with coarse-graining.

Microscopic (single-grid) vs Macroscopic (multi-grid)

I will consider an irradiation of a thin material by a pulsed light at normal incidence

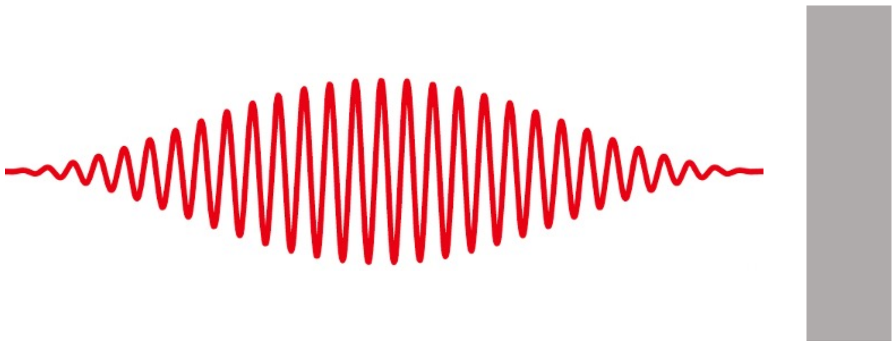

Microscopic (Single-scale) vs. Macroscopic (Multi-scale)

Microscopic Maxwell+TDDFT

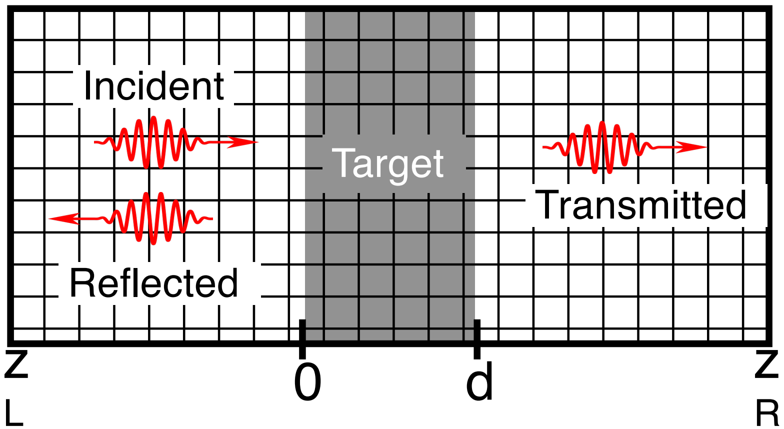

$$i\frac{\partial}{\partial t}u_{n\mathbf{k}} = \hat{H}_{\mathbf{k}+\frac{1}{c}A(\mathbf{r},t)}u_{n\mathbf{k}}$$

$$\left(\frac{1}{c^2}\frac{\partial^2}{\partial t^2} - \nabla^2\right)\mathbf{A}(\mathbf{r},t) + \frac{1}{c}\nabla\dot{\phi}(\mathbf{r},t) = -\frac{4\pi}{c}\mathbf{j}_e(\mathbf{r},t)$$

$$\nabla^2\phi(\mathbf{r},t) = 4\pi n_e(\mathbf{r},t)$$

Single-scale approach using a common spatial grid

nonlocal + nonlinear

S. Yamada *et al*, PRB **98**, 245147 (2018).

Macroscopic Maxwell+TDDFT

$$\left(\frac{1}{c^2}\frac{\partial^2}{\partial t^2} - \frac{\partial^2}{\partial Z^2}\right)\mathbf{A}_Z(t) = \frac{4\pi}{c}\mathbf{J}_Z(t)$$

grid spacing ~ 10 nm

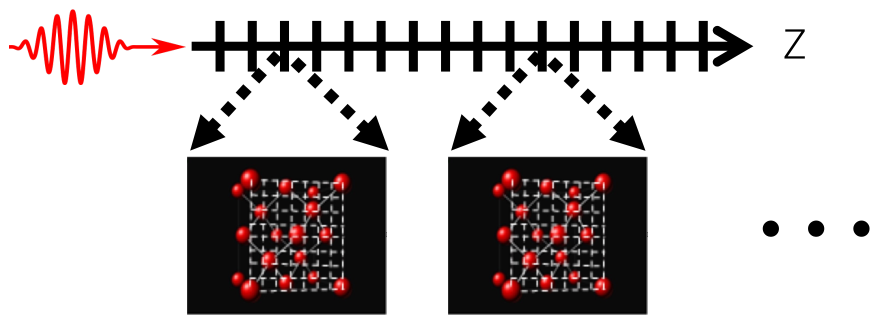

nm-scale grid #1

nm-scale grid #2

$$i\frac{\partial}{\partial t}u_{n\mathbf{k},Z} = \hat{H}_{\mathbf{k}+\frac{1}{c}A_Z(t)}u_{n\mathbf{k},Z}$$

$$i\frac{\partial}{\partial t}u_{n\mathbf{k},Z} = \hat{H}_{\mathbf{k}+\frac{1}{c}A_Z(t)}u_{n\mathbf{k},Z}$$

• • •

Multiscale approach using different spatial grid

nonlinear only

K. Yabana *et al.*, PRB **85**, 045134 (2012).

Microscopic (single-scale) Maxwell-TDDFT: pulsed light on Si nano-film

Shunsuke Yamada
Kansai Photon Sci. Inst

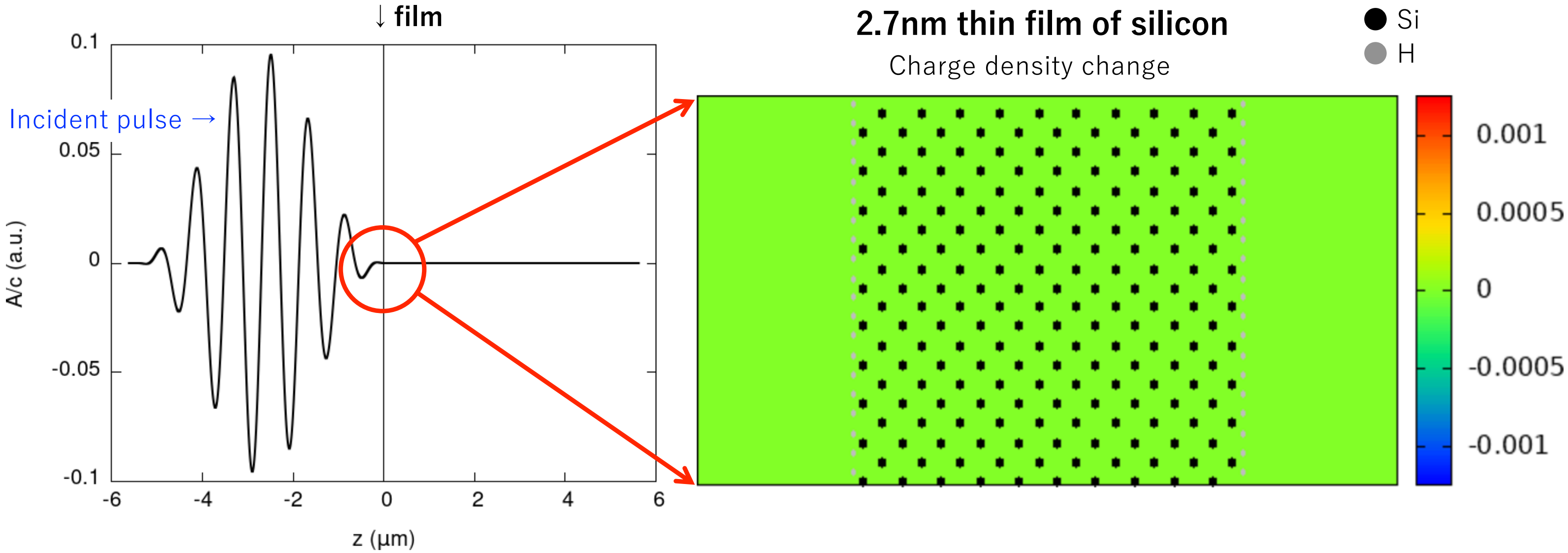

Light wavelength 800nm

Thicker film（27.2nm）

Light pulse: $\hbar\omega = 1.5\text{eV}, I = 10^{12}\text{W/cm}^2, T = 18\text{fs}$

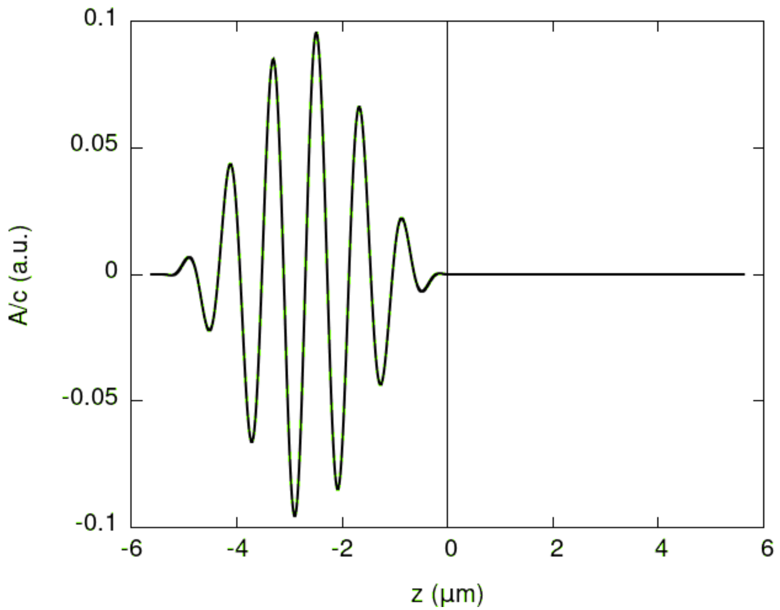

Charge density change

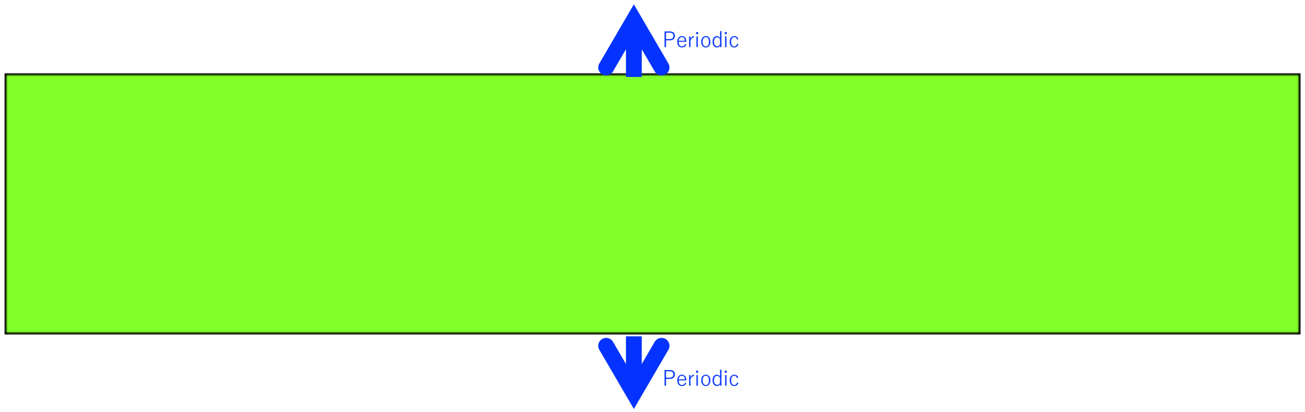

Max. possible thickness ~50nm limited by computational capability

Microscopic (Single-scale) vs. Macroscopic (Multi-scale)

Microscopic Maxwell+TDDFT

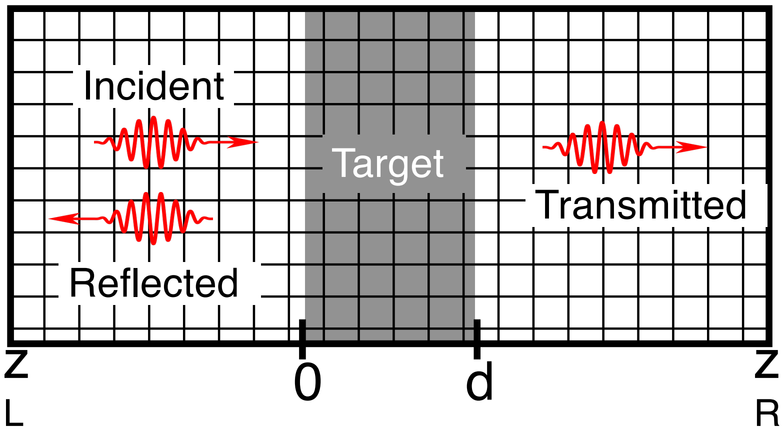

$$i\frac{\partial}{\partial t}u_{n\mathbf{k}} = \hat{H}_{\mathbf{k}+\frac{1}{c}A(\mathbf{r},t)}u_{n\mathbf{k}}$$

$$\left(\frac{1}{c^2}\frac{\partial^2}{\partial t^2} - \nabla^2\right)\mathbf{A}(\mathbf{r},t) + \frac{1}{c}\nabla\dot{\phi}(\mathbf{r},t) = -\frac{4\pi}{c}\mathbf{j}_e(\mathbf{r},t)$$

$$\nabla^2\phi(\mathbf{r},t) = 4\pi n_e(\mathbf{r},t)$$

Single-scale approach using a common spatial grid

nonlocal + nonlinear

S. Yamada *et al*, PRB **98**, 245147 (2018).

Macroscopic Maxwell+TDDFT

$$\left(\frac{1}{c^2}\frac{\partial^2}{\partial t^2} - \frac{\partial^2}{\partial Z^2}\right)\mathbf{A}_Z(t) = \frac{4\pi}{c}\mathbf{J}_Z(t)$$

grid spacing ~ 10 nm

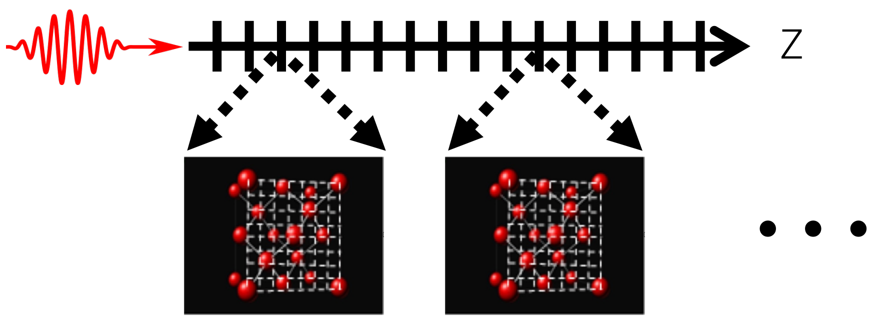

nm-scale grid #1 nm-scale grid #2

$$i\frac{\partial}{\partial t}u_{n\mathbf{k},Z} = \hat{H}_{\mathbf{k}+\frac{1}{c}A_Z(t)}u_{n\mathbf{k},Z}$$

$$i\frac{\partial}{\partial t}u_{n\mathbf{k},Z} = \hat{H}_{\mathbf{k}+\frac{1}{c}A_Z(t)}u_{n\mathbf{k},Z}$$

• • •

Multiscale approach using different spatial grid

nonlinear only

K. Yabana *et al.*, PRB **85**, 045134 (2012).

Macroscopic (multi-scale) Maxwell-TDDFT: pulsed light on 1μm Si film

Change of electron density from ground state

$\Delta n(\mathbf{r},t) = n(\mathbf{r},t) - n_{GS}(\mathbf{r})$

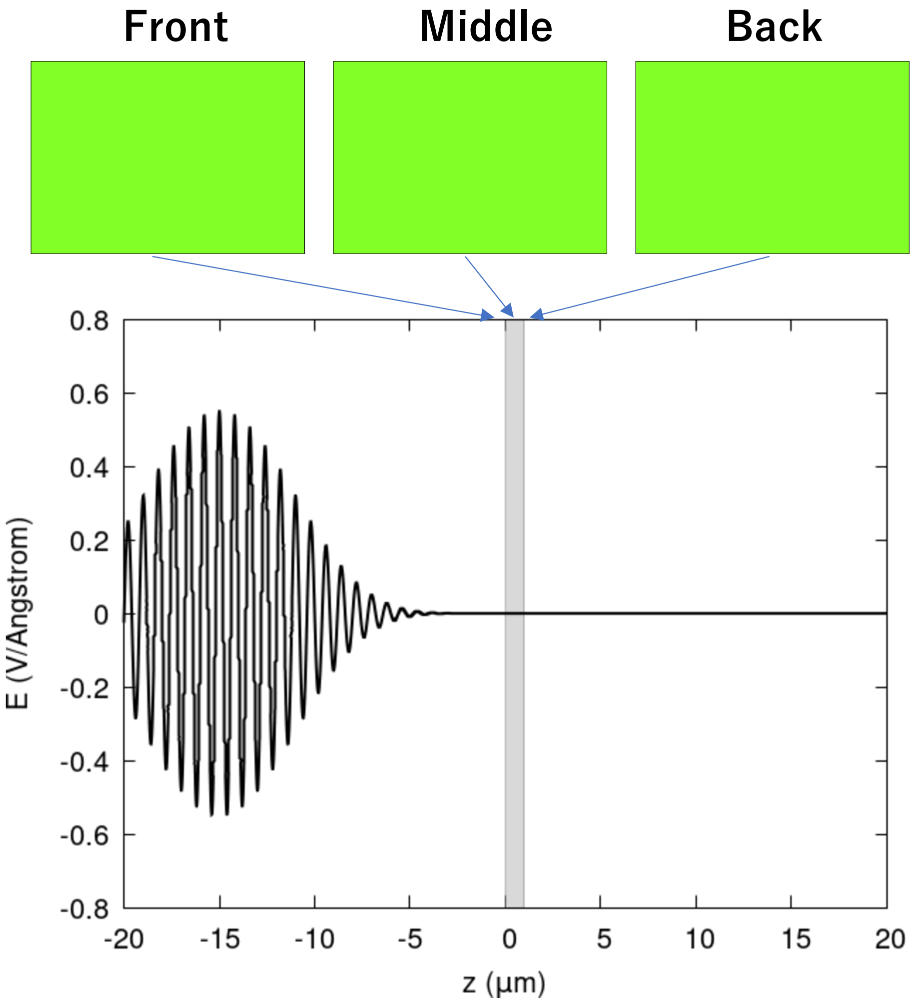

~200 grid points for 1μm film

Thin film
Silicon, 1 μm thick

Laser pulse
800nm (1.55eV=below gap)
4×10^{12} W/cm^2

Macroscopic (multi-scale) Maxwell-TDDFT: pulsed light on 1μm Si film

Change of electron density from ground state

$\Delta n(\mathbf{r},t) = n(\mathbf{r},t) - n_{GS}(\mathbf{r})$

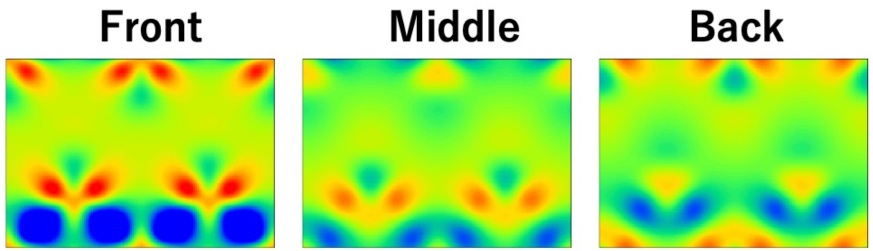

~200 grid points for 1μm film

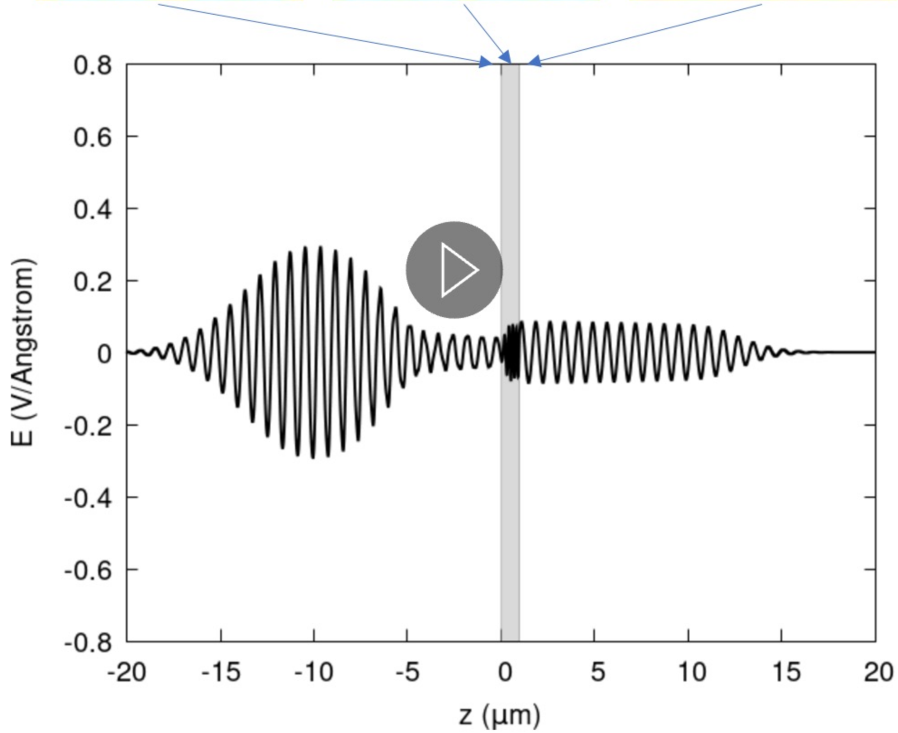

Thin film
Silicon, 1 μm thick

Laser pulse
800nm (1.55eV=below gap)
4×10^{12} W/cm^2

Today I will talk on:

- **Solve Maxwell and Schrödinger (time-dependent Kohn-Sham) equations simultaneously.**
- **Directly connecting electromagnetism and quantum mechanics.**

Classical electromagnetic fields

$$\nabla \times \nabla \times \mathbf{A} + \frac{1}{c^2}\frac{\partial^2}{\partial t^2}\mathbf{A} = \frac{4\pi}{c}\mathbf{j}$$

Quantum electronic motion

$$i\hbar\frac{\partial}{\partial t}\psi_i = \left\{ \frac{1}{2m}\left(-i\hbar\nabla + \frac{e}{c}\mathbf{A}\right)^2 + V_{ion} + V_H + V_{xc} \right\}\psi_i$$

$$\mathbf{j} = -\frac{e}{2m}\left\{\psi_i^*\left(-i\hbar\nabla + \frac{e}{c}\mathbf{A}\right)\psi_i + c.c.\right\}$$

- **Why and where it is necessary?**
- **How it is carried out?**
- **How it works?**

High intensity laser pulse on various materials : Systematics

Strong pulsed light irradiates on solid surface.

Reflection and absorption take place.

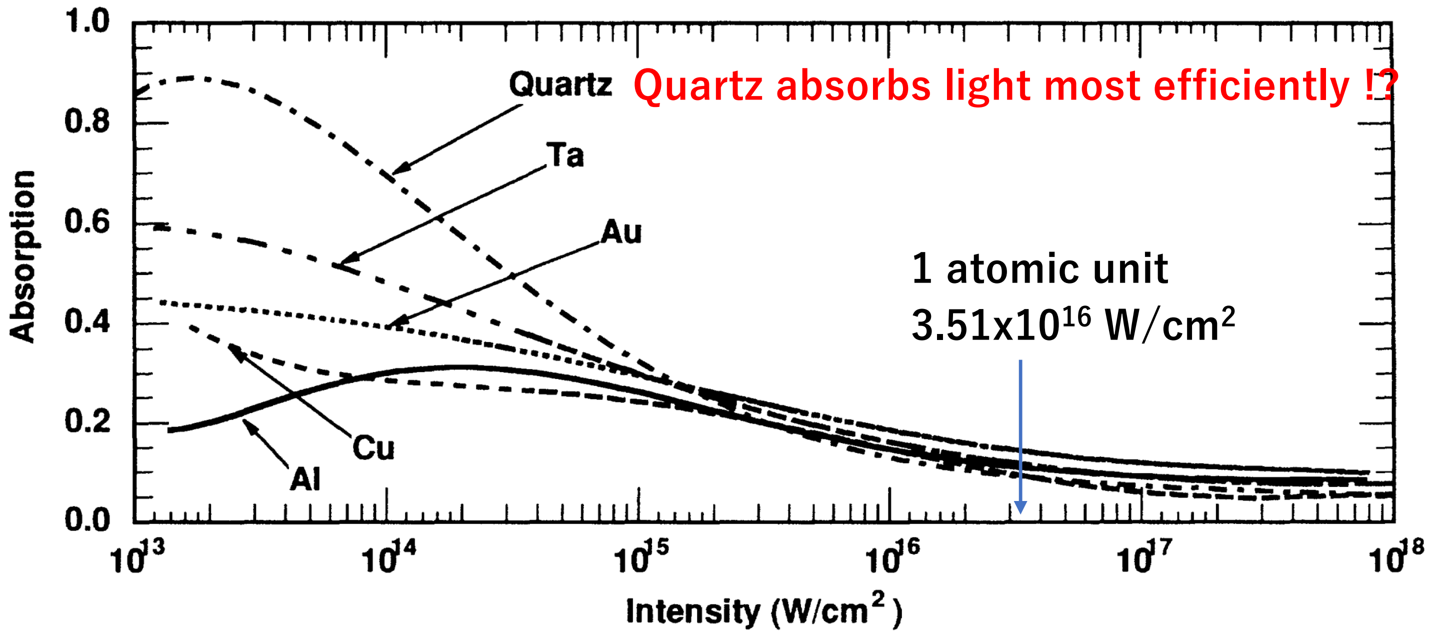

Experiment at LLNL, using 120fs pulse D.F.Price et al., *Phys.Rev.Lett.* **75**,252 (1995)

Atsushi Yamada
Defence Academy

High intensity laser pulse on various materials : Systematics

Experiment at LLNL, using 120fs pulse

D.F.Price et al., *Phys.Rev.Lett.* **75**,252 (1995)

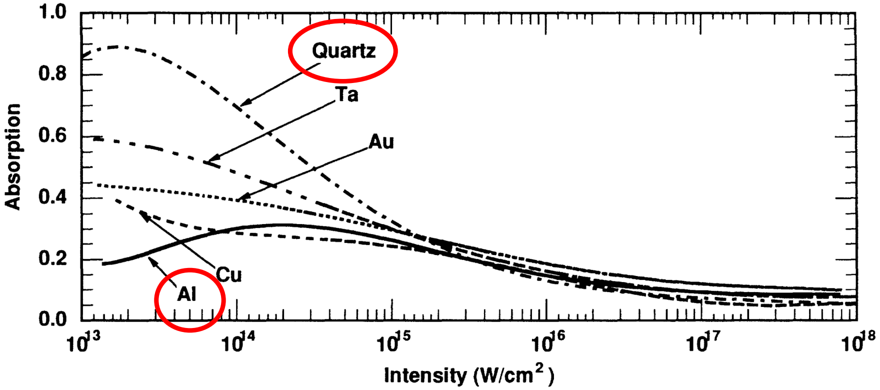

FIG. 1. Absorption fraction vs peak laser intensity for aluminum, copper, gold, tantalum, and quartz targets. In Figs. 1, 3, 4, and 5 laser intensity is the temporal and spatial peak value of the laser intensity.

Multiscale Maxwell-TDDFT calculation

A. Yamada, K. Yabana, Phys. Rev. B109, 245130 (2024)

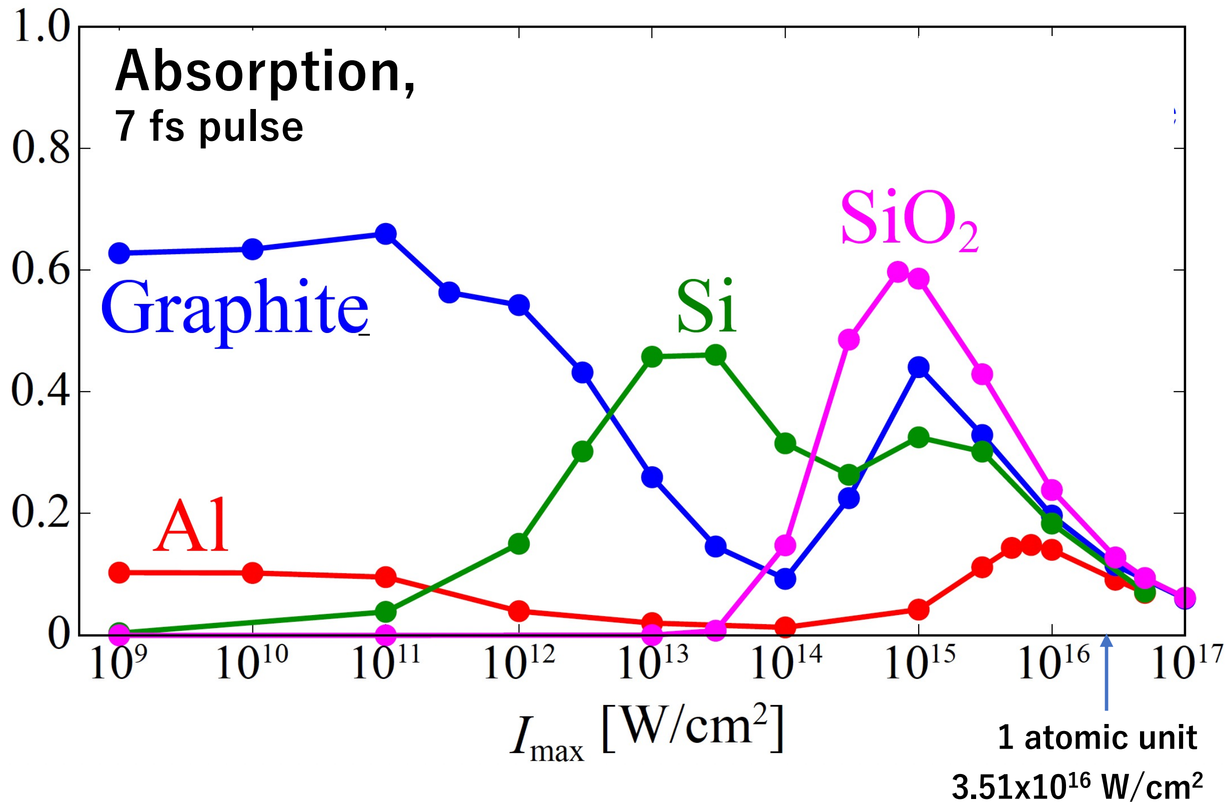

Nonlinear optical response: Mechanisms

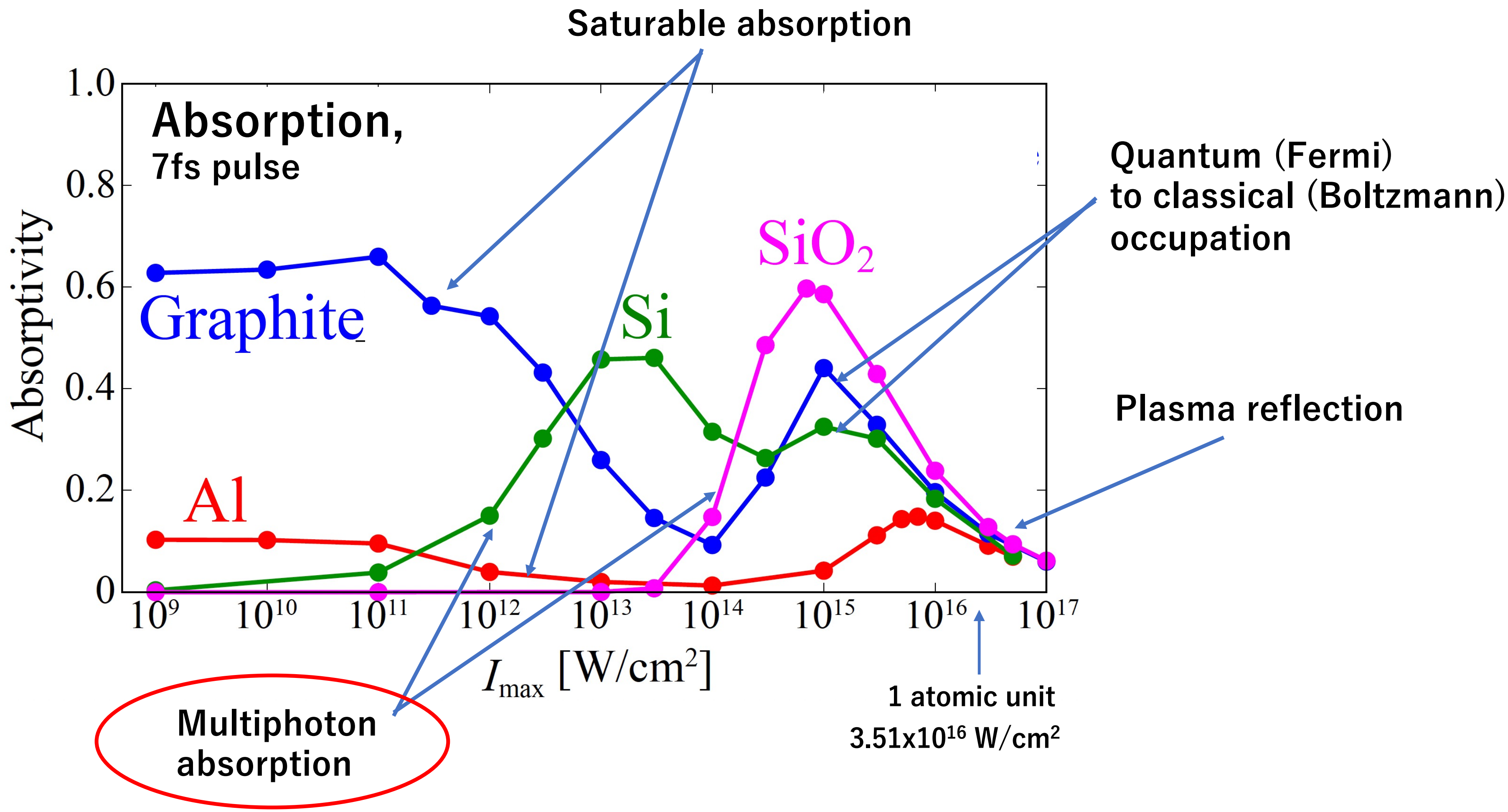

At which intensity of light, glass starts to absorb light?

Laser processing of dielectrics

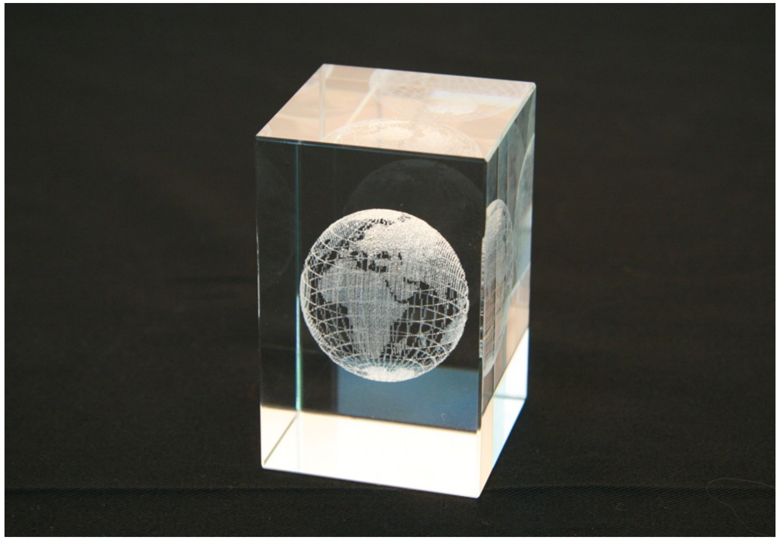

Calculation for SiO_2 (alpha-quartz)

Laser pulse propagation through SiO_2 10μm thin film

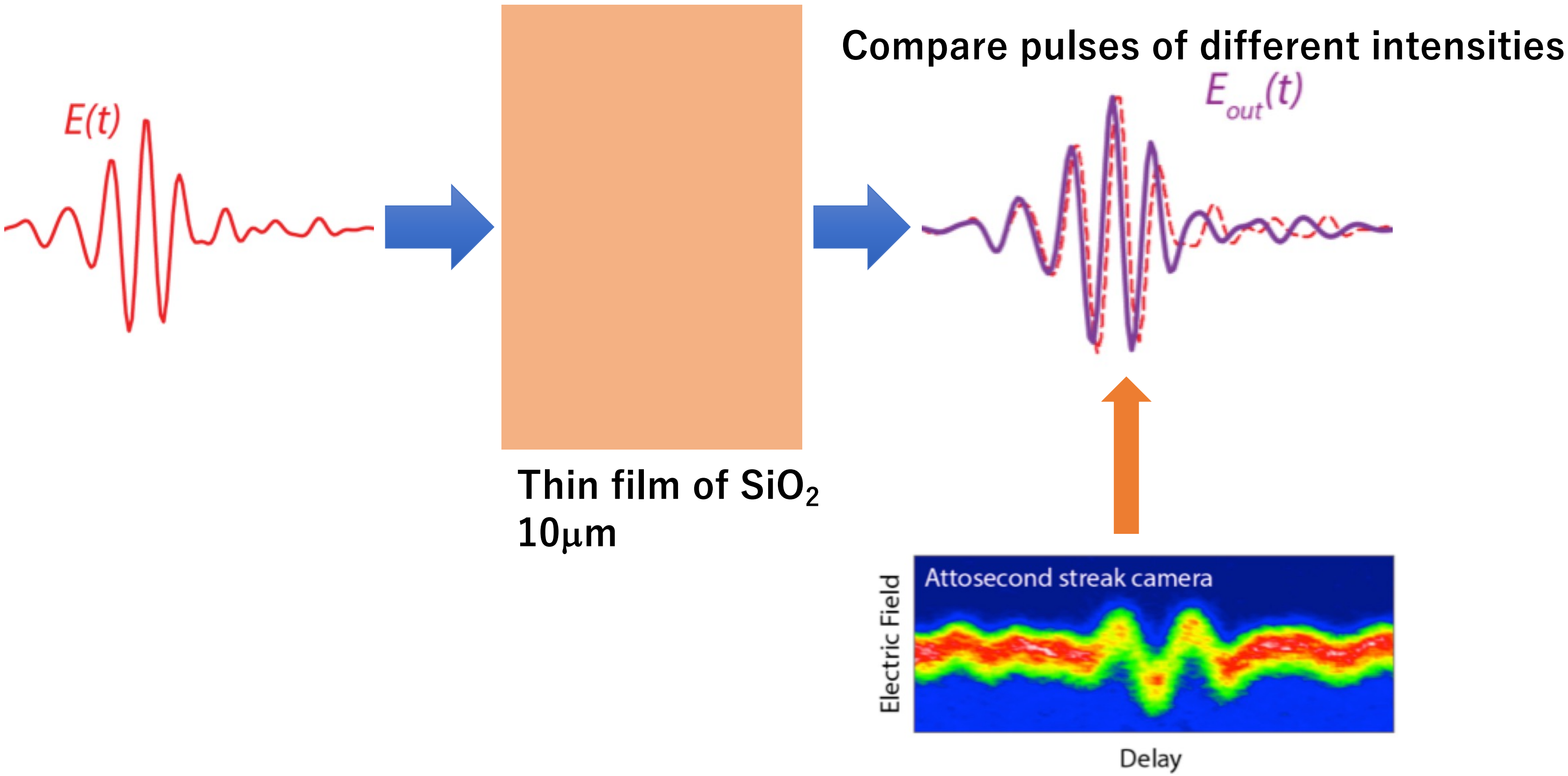

EXP: Attosecond streaking measurements
by Max Planck Inst. Quantum Optics

Maxwell + TDDFT multiscale simulation : 10 μm SiO_2

Laser electric field, red (strong), blue (weak)

$\hbar\omega = 1.55\text{eV}$

$\lambda = 800\text{nm}$

$\text{I} = 7 \times 10^{13} \text{W/cm}^2$

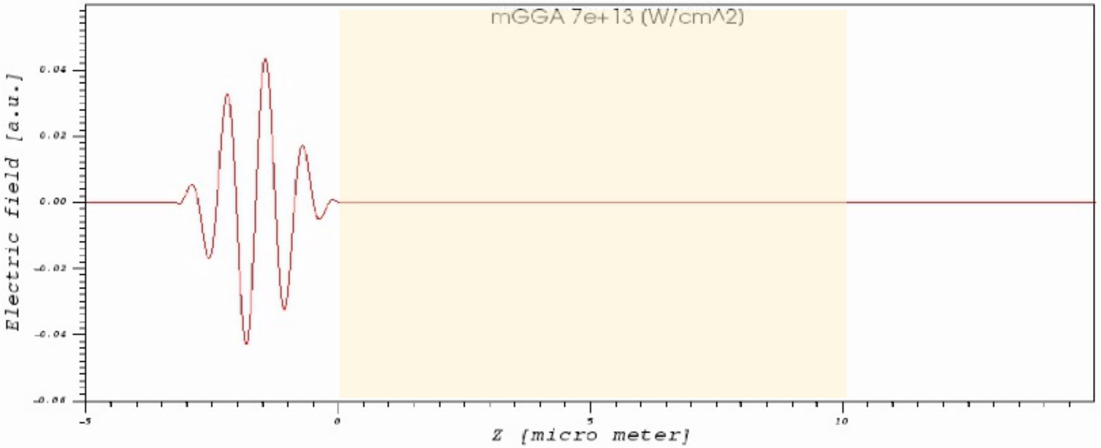

Energy transfer from laser pulse to electrons [eV/atom]

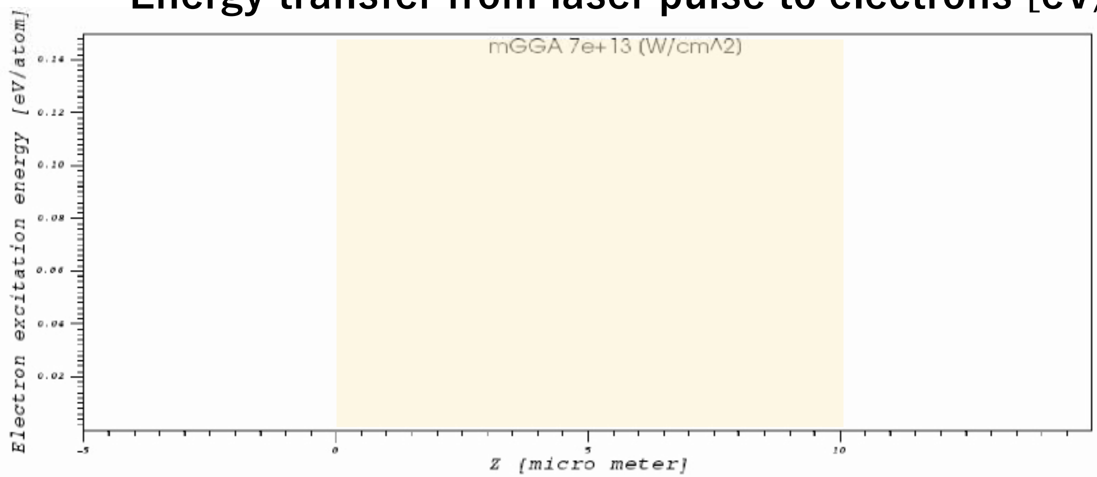

80,000 cores, 20 hours
at K-Computer, Kobe

Energy deposited to electrons in SiO_2
increases rapidly at a certain laser intensity

>> Damage threshold

Multiphoton/Tunneling excitation

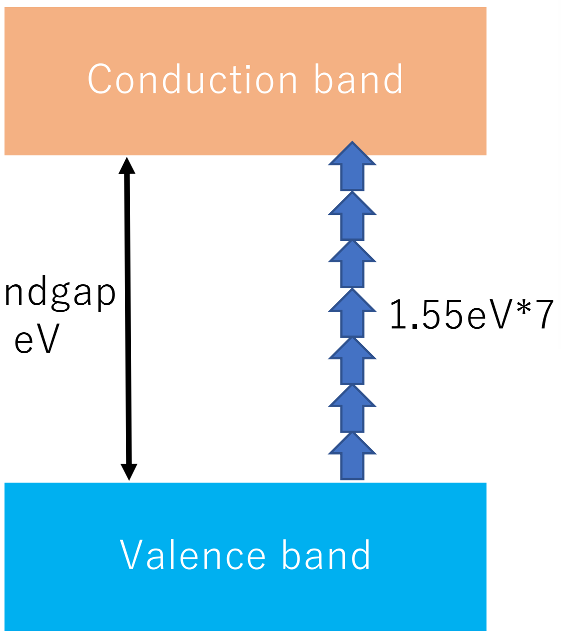

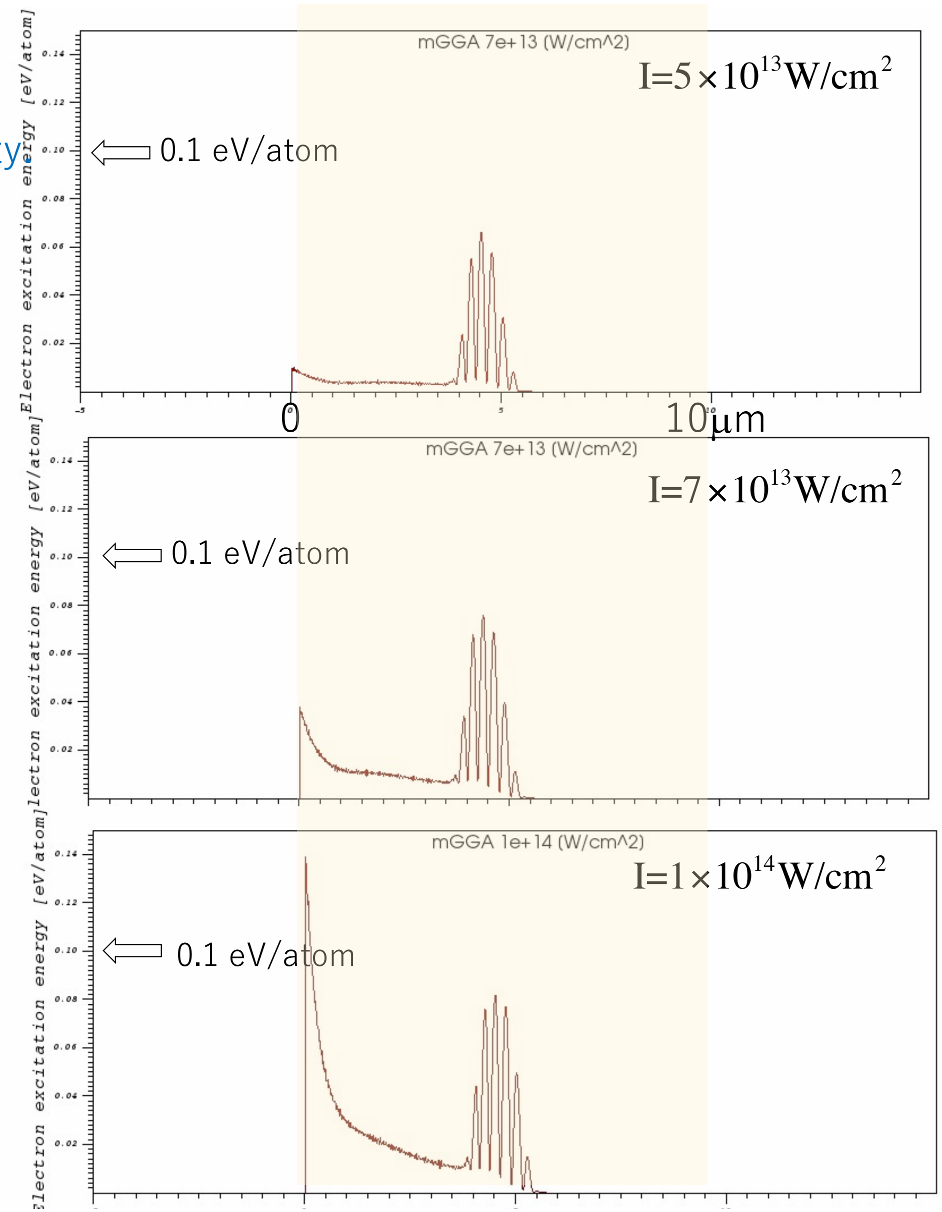

Shunsuke Sato
Tohoku U.

Comparison between theory and experiment

Energy deposition from laser pulse to SiO_2 at mid point (5μm)

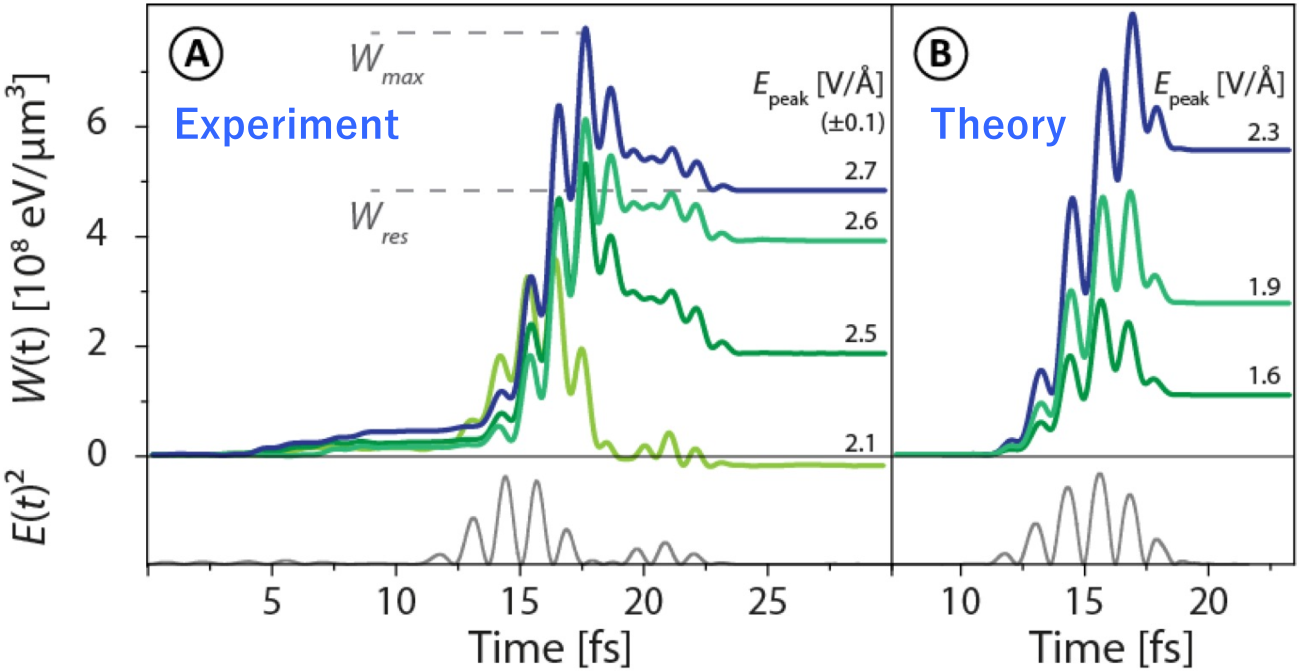

A. Sommer et.al, Nature 534, 86 (2016).
(EXP: Max Planck Institute for Quantum Optics)

Nonlinear optical response: Mechanisms

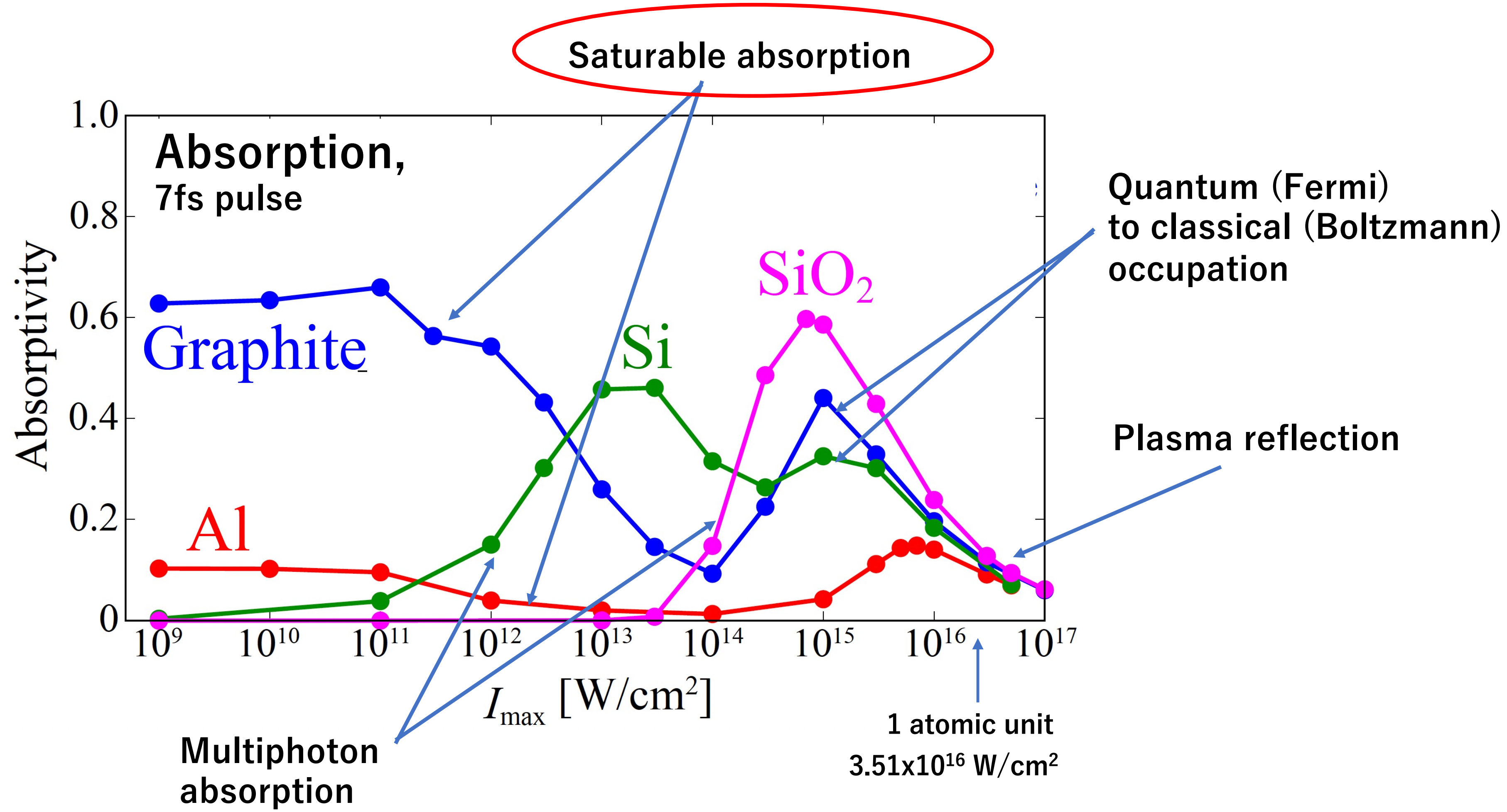

Tentative results

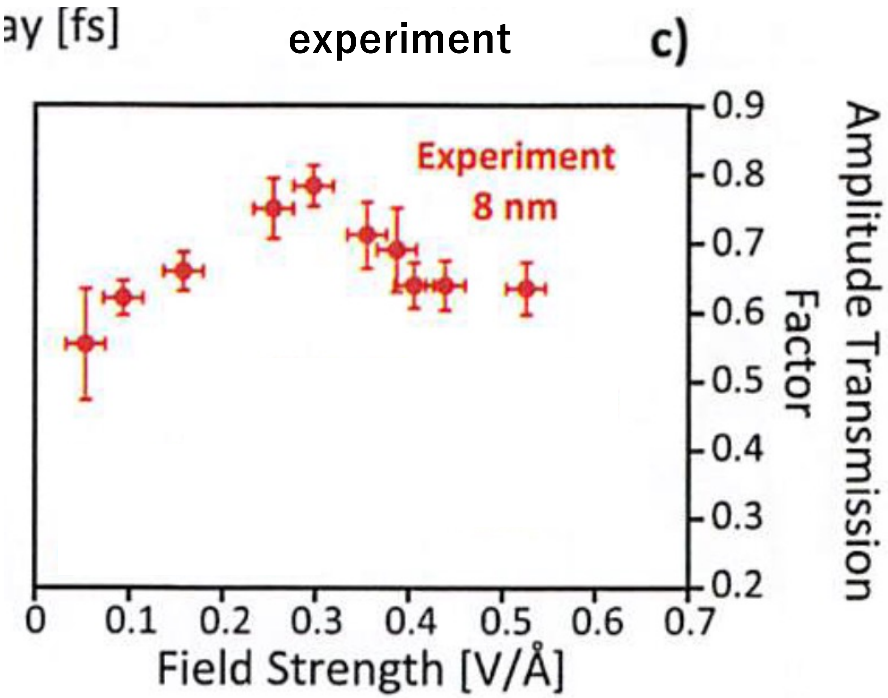

Oblique, multiscale Maxwell-TDDFT calculation

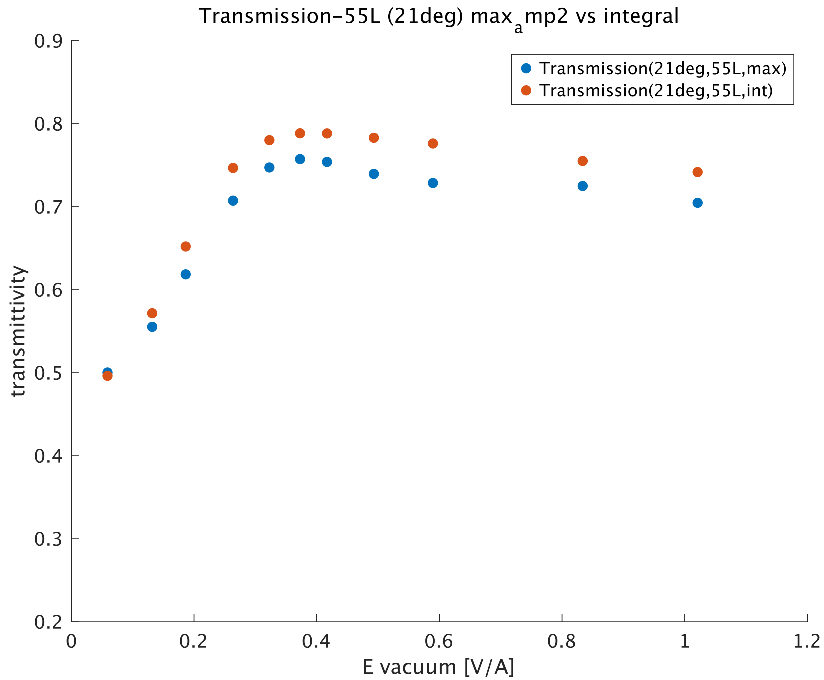

Nonlinear optical response: Mechanisms

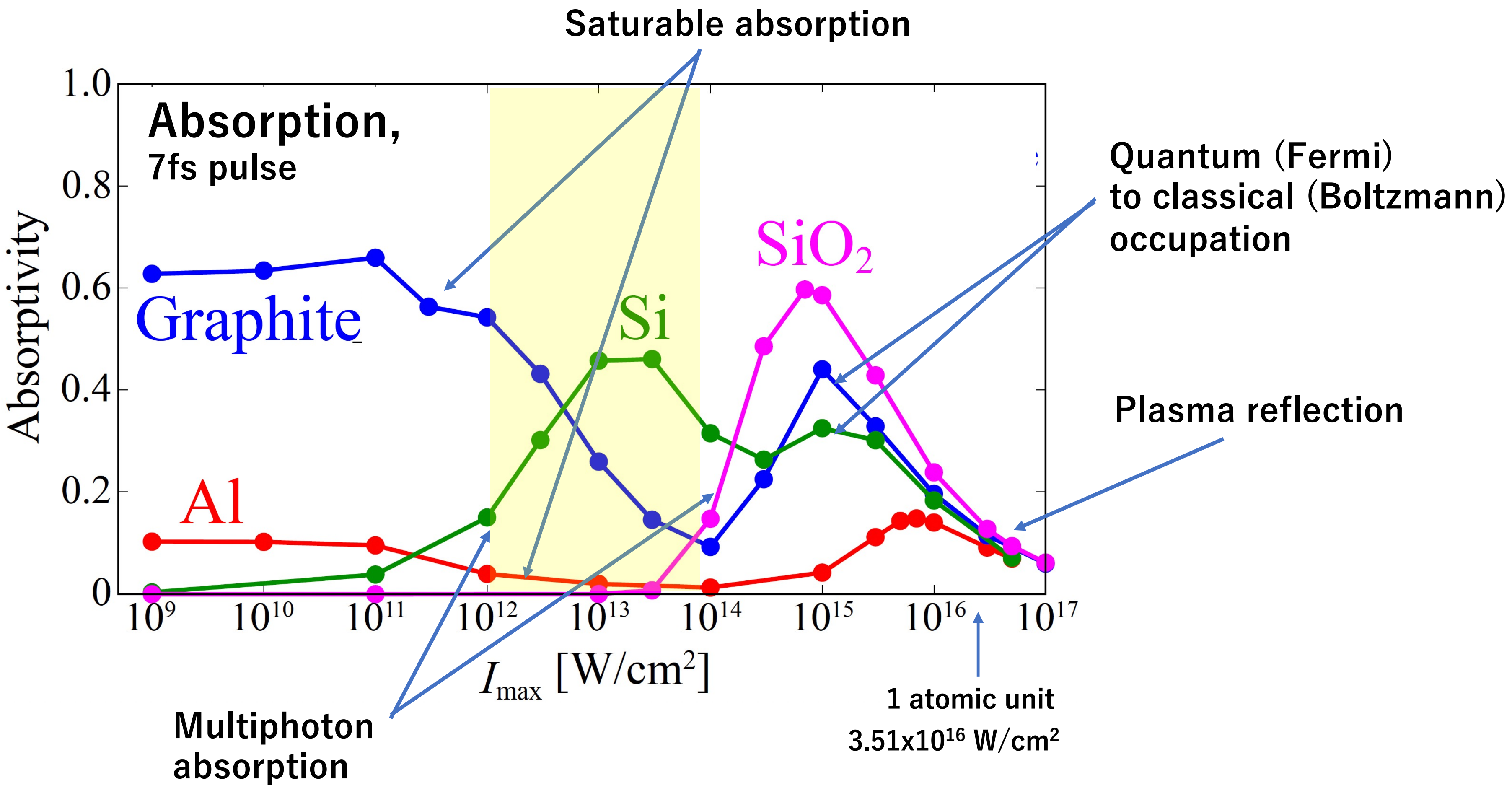

High harmonic generation (HHG)

High harmonic generation from atoms

Soft X-ray from visible light

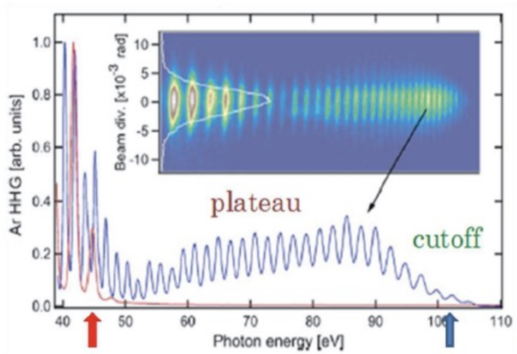

3 step model (electron rescattering)

P.B. Corkum, Phys. Rev. Lett. 71, 1994 (1993)

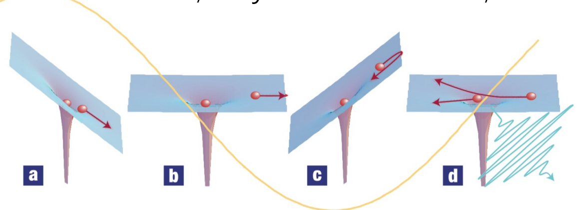

P.B. Corkum, F. Krausz, Nature Phys. 3, 380 (2007)

High harmonic generation from solids

Compact X-ray device?

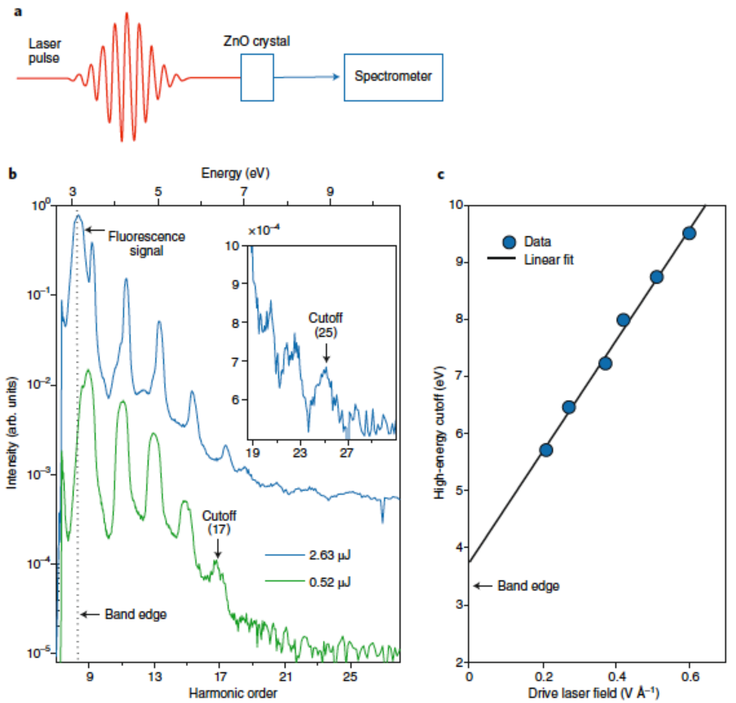

S. Ghimire et al, Nat. Phys. 7, 138 (2011)

S. Ghimire, D.A. Reis, Nature Physics 15, 10 (2019)

Macroscopic (multi-scale) Maxwell-TDDFT: pulsed light on 1μm Si film

Change of electron density from ground state
$\Delta n(\mathbf{r},t) = n(\mathbf{r},t) - n_{GS}(\mathbf{r})$

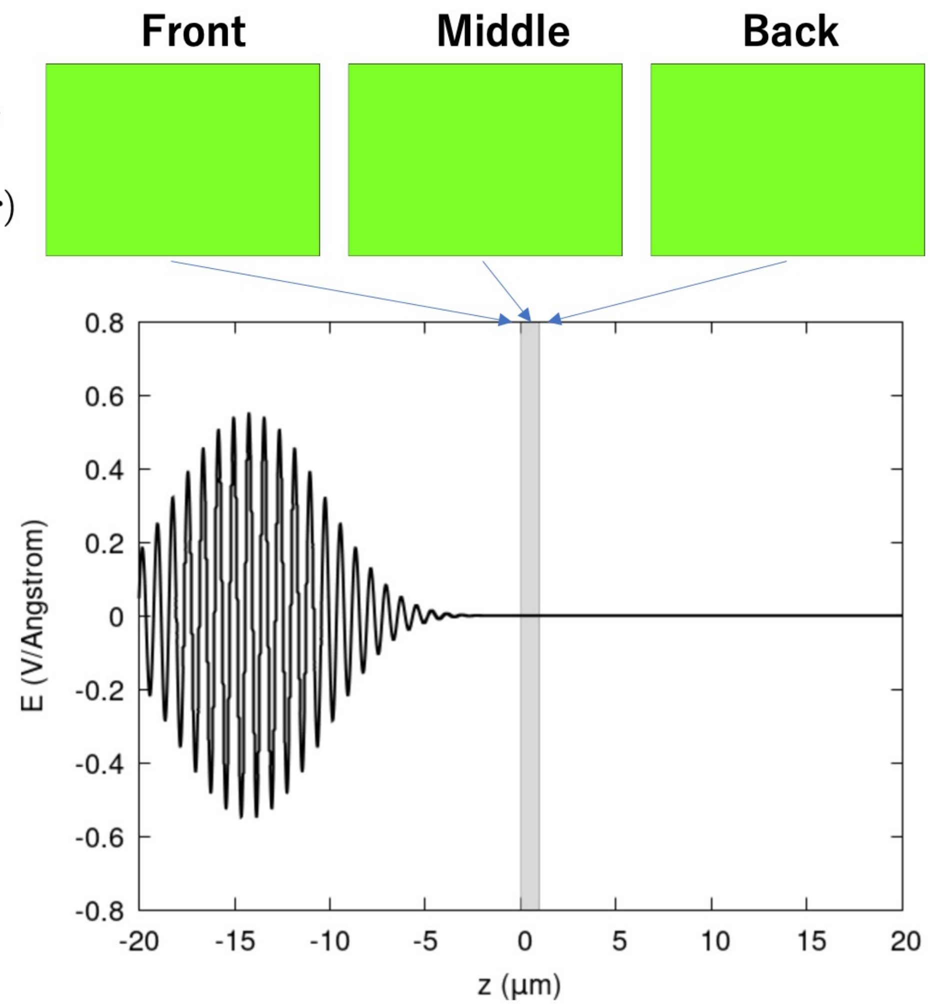

~200 grid points for 1μm film

Thin film
Silicon, 1 μm thick

Laser pulse
800nm (1.55eV=below gap)
4×10^{12}W/cm^2

High harmonic components in transmission/reflection waves

S. Yamada et.al, Phys. Rev. B107, 035132 (2023)

Thin film
Silicon, 1 μm thick

Laser pulse
800nm (1.55eV=below gap)
$4x10^{12}W/cm^2$

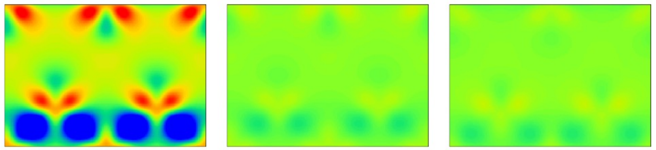

Flat envelope:
high field part was consumed for electronic excitation.

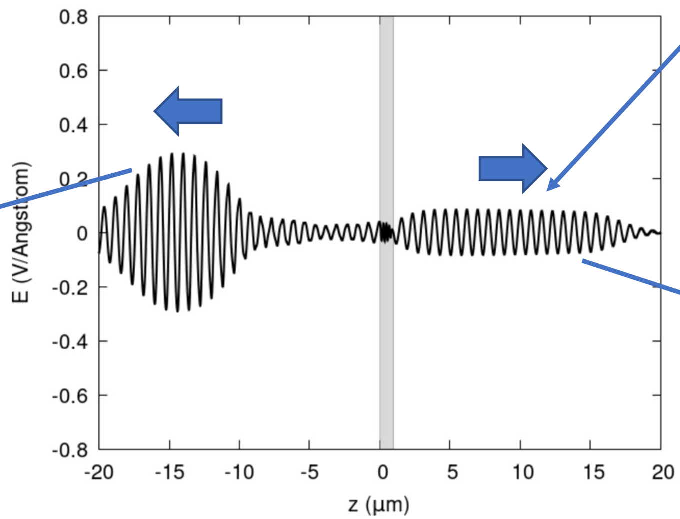

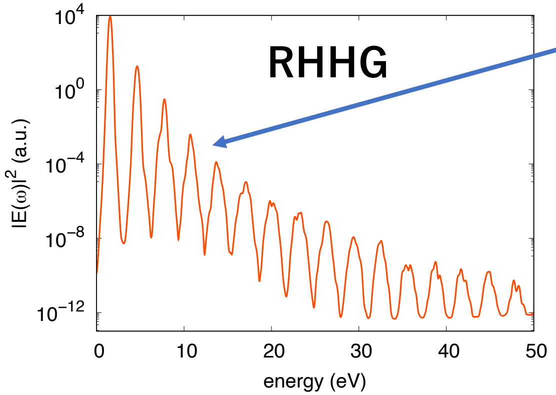

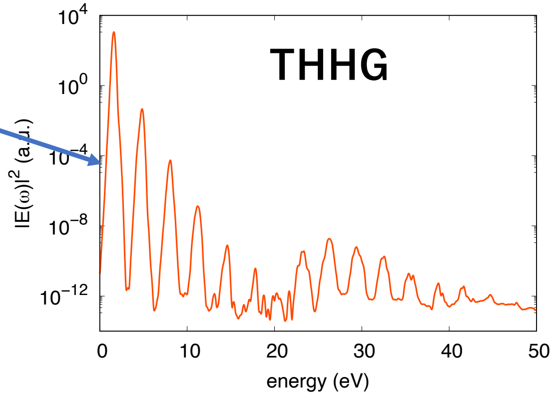

Where is HHG produced?

Front or back surfaces

S. Yamada et.al, PRB107, 035132 (2023)

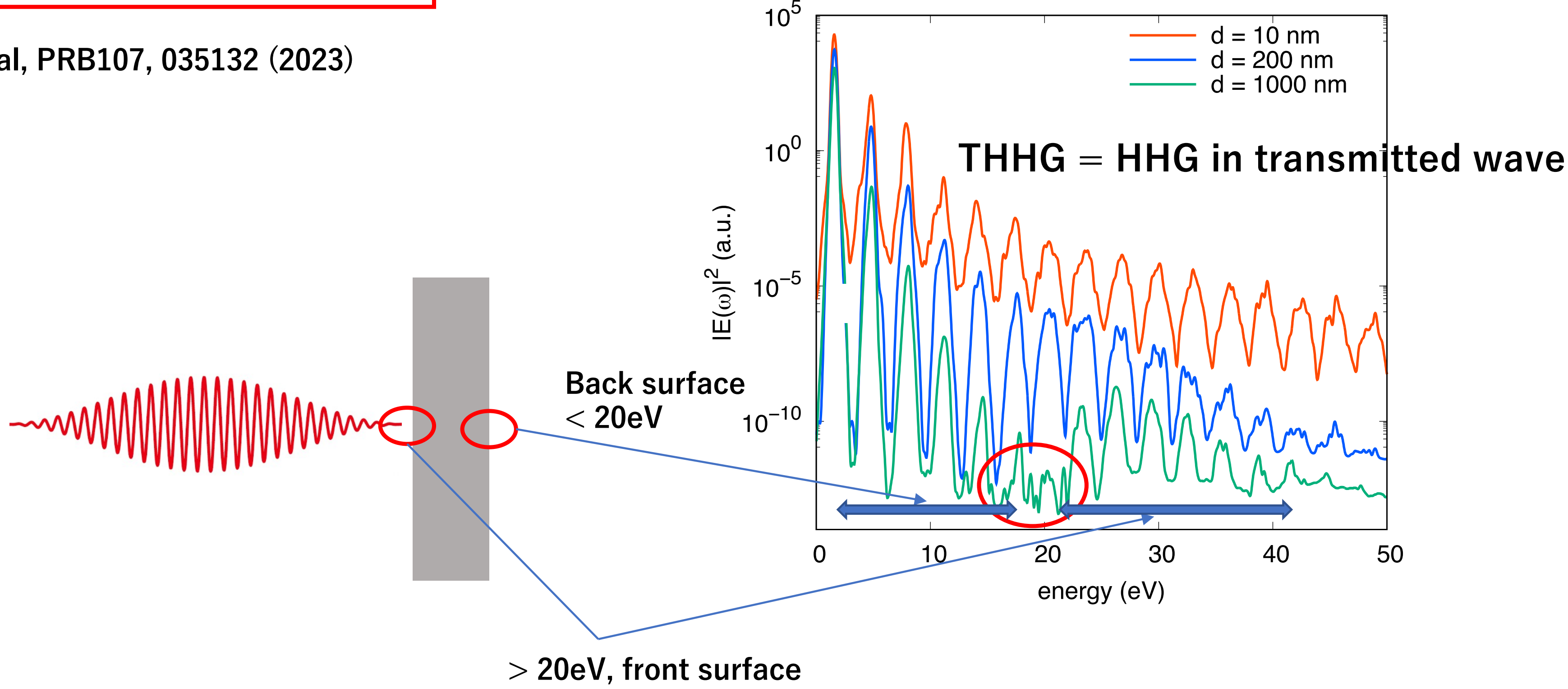

What is the most efficient thickness to produce strong HHG?

5~20nm

S. Yamada, K. Yabana, Phys. Rev. B103, 155426 (2021)

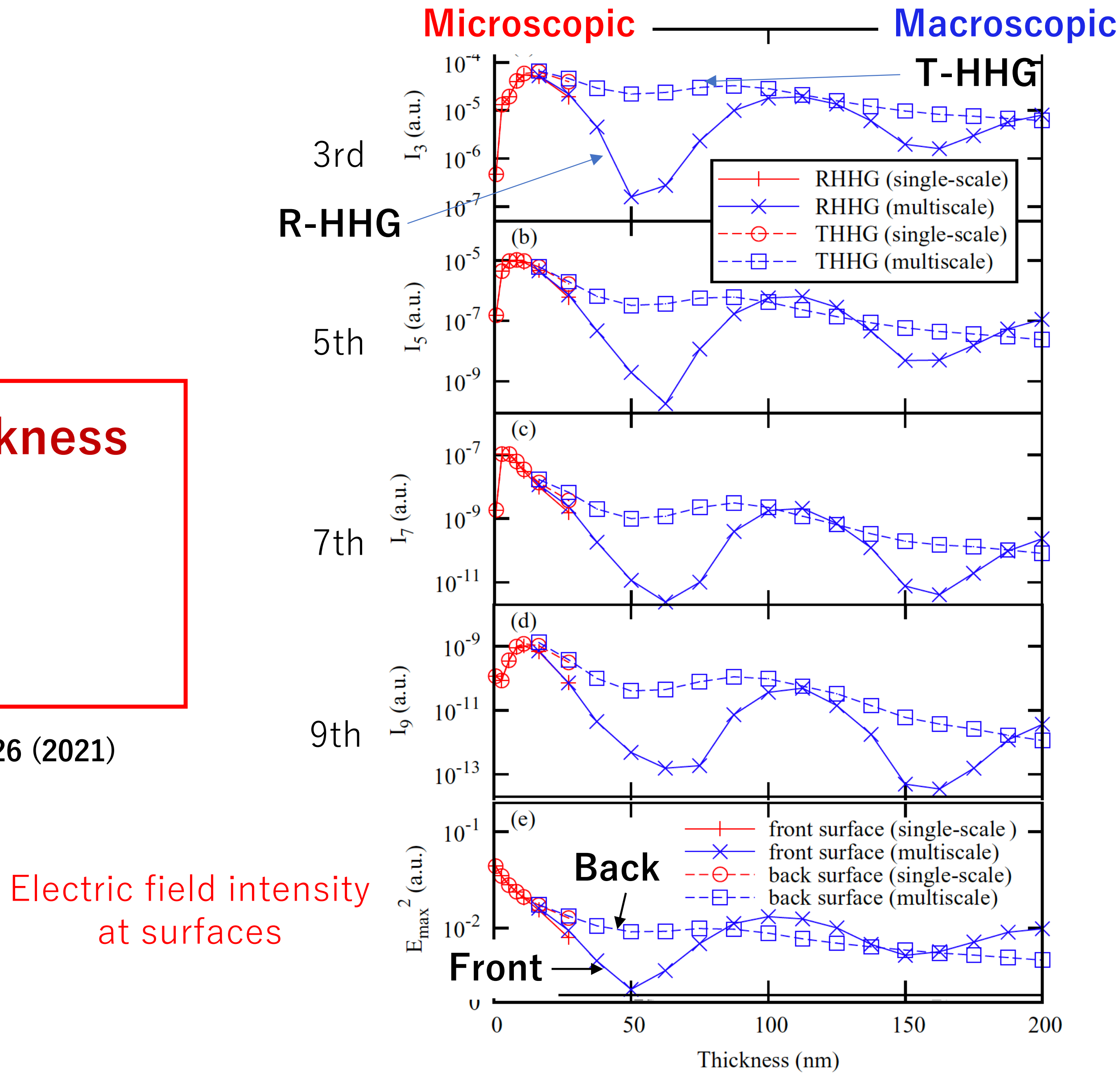

Nano-plasmonics and nonlocality

Color change of Au nano-particles

Electron spill-out at the surface
due to quantum effect

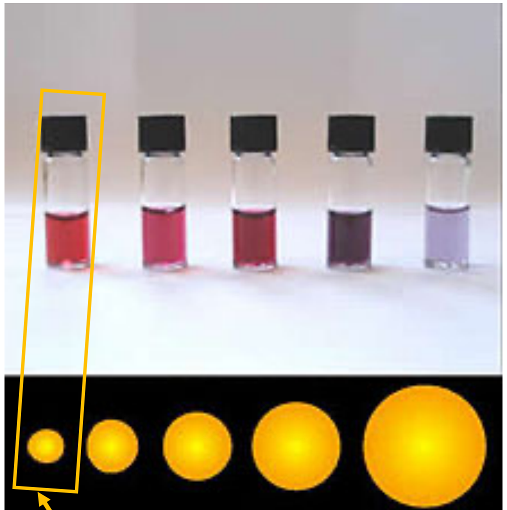

~10nm (red color)

$$\omega_M{}^2 = \frac{4\pi n e^2}{3m}$$

Optical absorption of nano-dimer

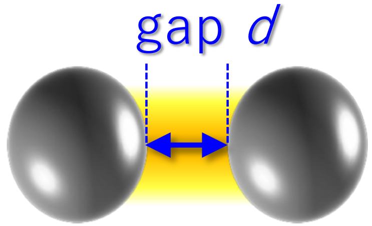

J.A. Scholl et.al,
Nano Lett. 13, 564 (2013)

Quantum tunneling between nano-particles affects response

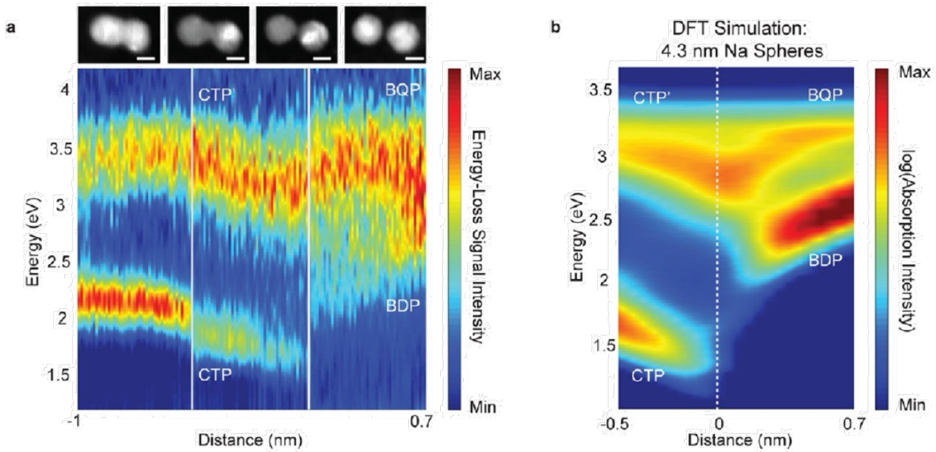

Figure 4. Continuous EELS collection to observe quantum tunneling effects at small gap sizes for silver spheres and theoretical comparison with sodium spheres. (a) A STEM-EELS probe enables particle motion during EEL spectra collection of a 9-nm-diameter silver homodimer. STEM images collected at the beginning and end of each scan (bounded by solid vertical lines) indicate the separation distances (+0.7, < 0.27, −0.3, and −1.0 nm). (b) DFT simulation of the plasmonic response of 4.3-nm-diameter sodium spheres in vacuum from recent work,[13] with particle separation between +0.7 and −0.5 nm. The spectra from both experiment and theory exhibit a diminished BDP resonance peak at separations of only a few angstroms, indicating quantum tunneling. The charge transfer mode appears after particle contact. Image scale bars equal 5 nm.

Optical response of plasmonic meta-surface with sub-nm gap

T. Takeuchi, M. Noda, K. Yabana, ACS Photonics 6, 2517 (2019).
T. Takeuchi, K. Yabana, Scientific Reports 10, 21270 (2020).

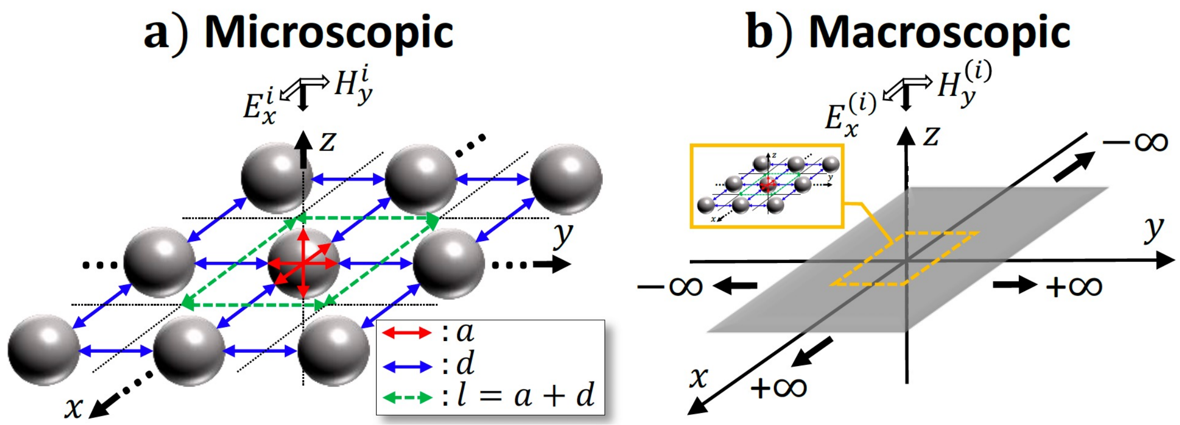

Maxwell eq. for light propagation in 2D approx.

$$\frac{1}{c^2}\frac{\partial^2}{\partial t^2}A(z,t) - \frac{\partial^2}{\partial z^2}A(z,t) = \frac{4\pi}{c}I(z,t) \qquad I(z,t) = \delta(z)\tilde{I}(t)$$

TDDFT for electronic motion in jellium approx.

$$i\frac{\partial u_{n\mathbf{k}}(\mathbf{r},t)}{\partial t} = \left[\frac{1}{2}\left(-i\nabla + \mathbf{k} + \frac{1}{c}\mathbf{A}(t)\right)^2 - \phi(\mathbf{r},t) + V_{\mathrm{XC}}(\mathbf{r},t)\right]u_{n\mathbf{k}}(\mathbf{r},t)$$

Optical response of plasmonic meta-surface with sub-nm gap

Takashi Takeuchi
RIKEN (former affiliation)

Nano-particle:
3nm radius, 398 electrons

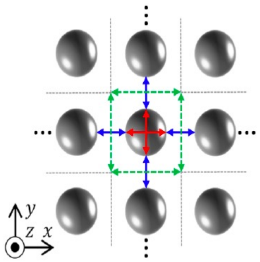

Linear absorption

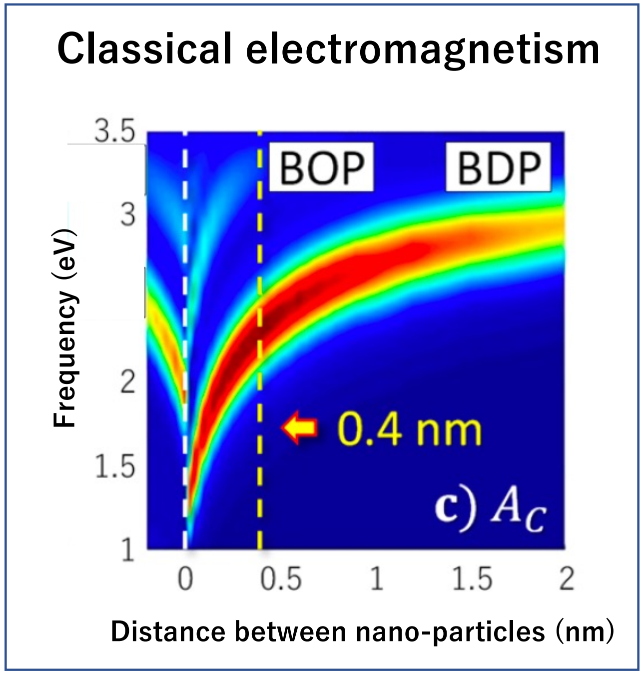

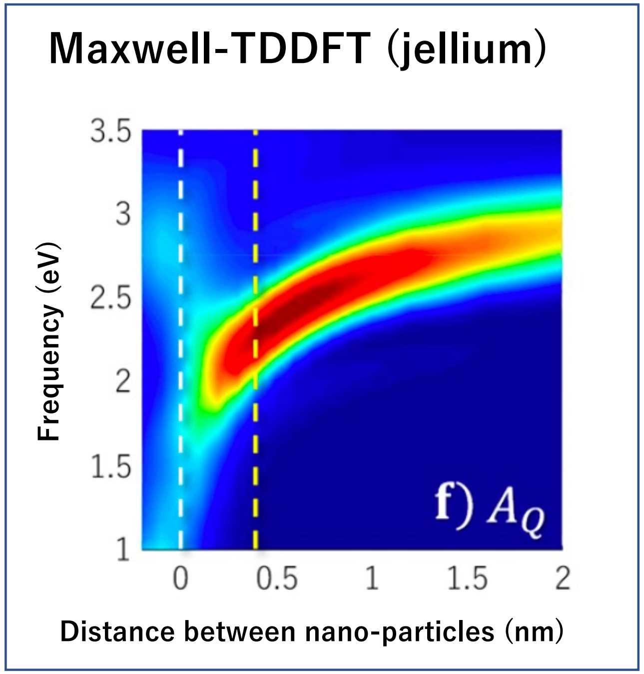

Quantum effect:
Plasmon becomes diffuse
as two particles come close (<0.2nm)

T. Takeuchi et.al, ACS Photonics 6, 2517 (2019)

Recent experimental measurement (B. Lu et.al, ACS Nano 17, 12774 (2023).)

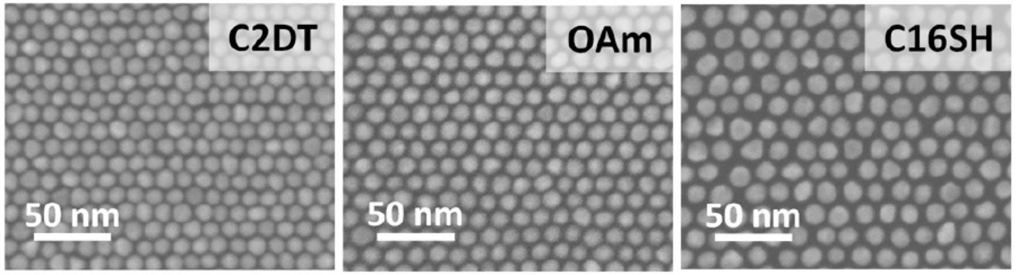

Meta-surface of Au nanoparticles (nano-particle distance as small as 0.1nm)

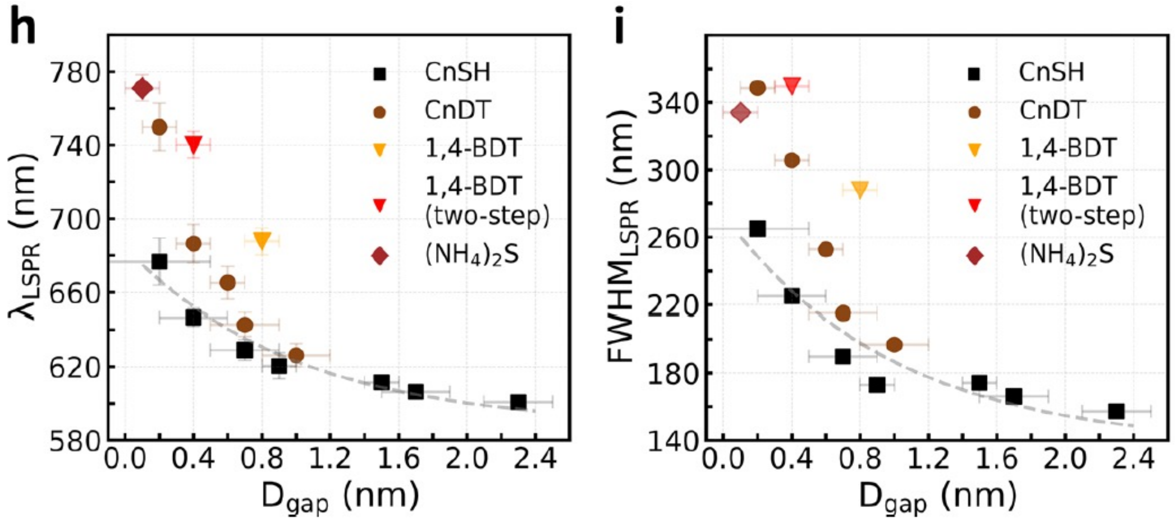

Strong red-shift of absorption as the gap distance decreases.

An irradiation of a thin material by a pulsed light at oblique incidence

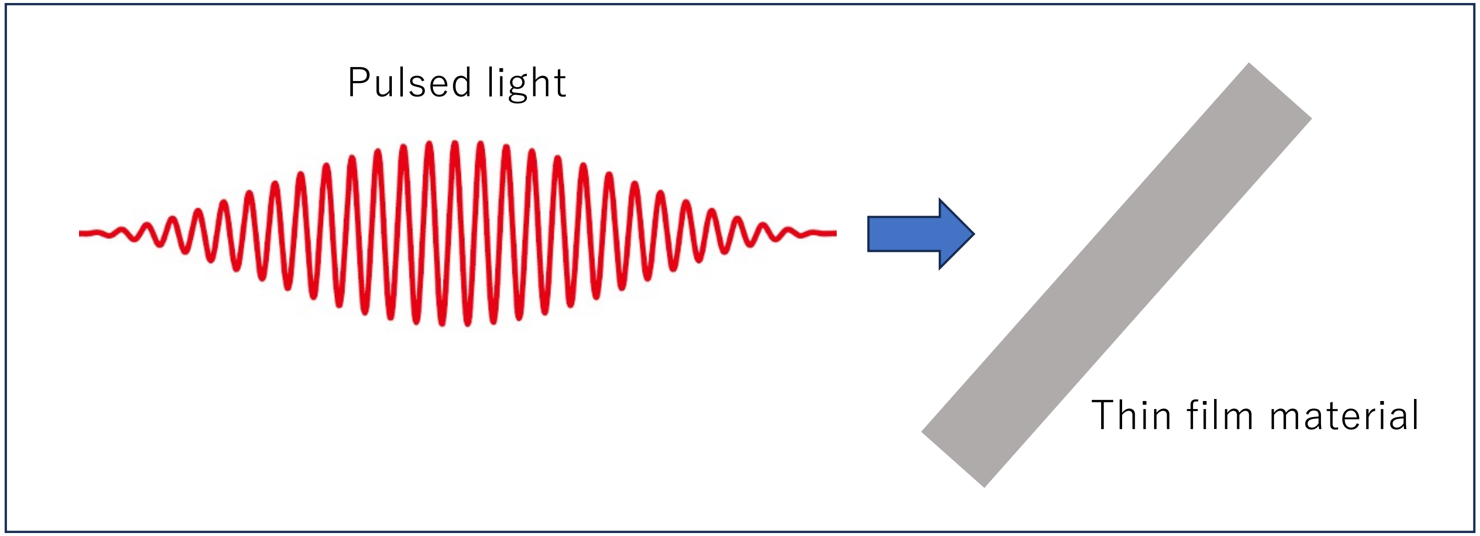

- **Weak pulse case :**
  macroscopic electromagnetism

- **Strong pulse case :**
  macroscopic electromagnetism + TDDFT for electron dynamics

Multiscale Maxwell-TDDFT calculation at oblique incidence

M. Uemoto, K. Yabana, Opt. Exp. 30, 23664 (2022), K. Yabana et.al, in preparation

$\theta = 60^\circ$

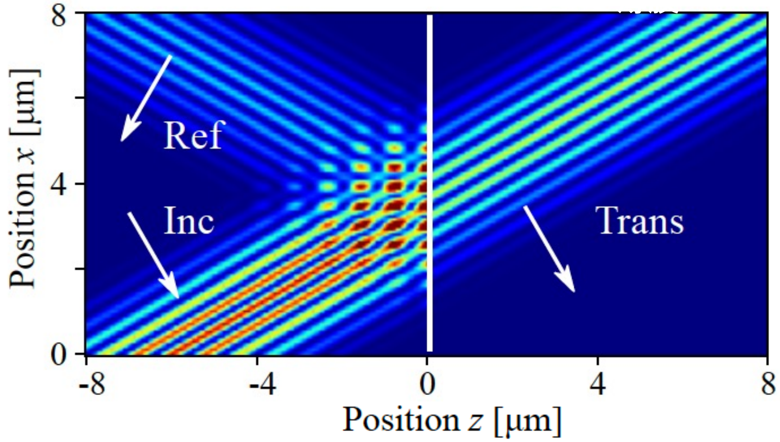

Translational symmetry involving time and space

$$\boldsymbol{A}(\boldsymbol{R},t) = \boldsymbol{a}\left(Z, t - \frac{X\sin\theta}{c}\right)$$

$$\boldsymbol{J}(\boldsymbol{R},t) = \boldsymbol{j}\left(Z, t - \frac{X\sin\theta}{c}\right)$$

functions of z and t only

There appears no dangerous term like (d/dz)p_z

$$\nabla\times\boldsymbol{B} = \frac{4\pi}{c}\boldsymbol{J} + \frac{1}{c}\frac{\partial}{\partial t}\boldsymbol{E},$$

$$\nabla\times\boldsymbol{E} + \frac{1}{c}\frac{\partial}{\partial t}\boldsymbol{B} = 0,$$

***s*-polarization**

$$\frac{\cos^2\theta}{c}\frac{\partial}{\partial t}e_y(z,t) = \frac{\partial}{\partial z}b_x(z,t) - \frac{4\pi}{c}j_y(z,t)$$

$$\frac{1}{c}\frac{\partial}{\partial t}b_x(z,t) = \frac{\partial}{\partial z}e_y(z,t)$$

***p*-polarization**

$$\frac{1}{c}\frac{\partial}{\partial t}e_x(z,t) = -\frac{\partial}{\partial z}b_y(z,t) - \frac{4\pi}{c}j_x(z,t)$$

$$\frac{\cos^2\theta}{c}\frac{\partial}{\partial t}b_y(z,t) = -\frac{\partial}{\partial z}e_x(z,t) + \frac{4\pi}{c}\sin\theta j_z(z,t)$$

Oblique incidence can be calculated with the same computational cost as normal incidence.

Oblique-incident light propagation: linear optics

s- and p-polarizations

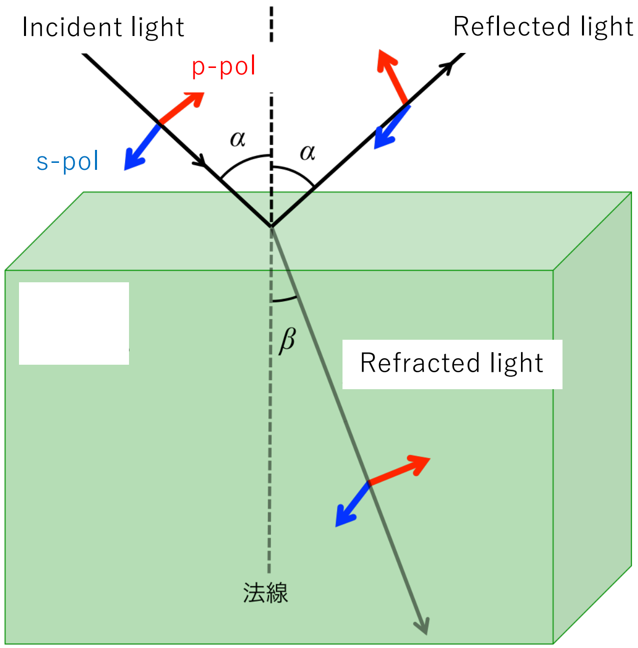

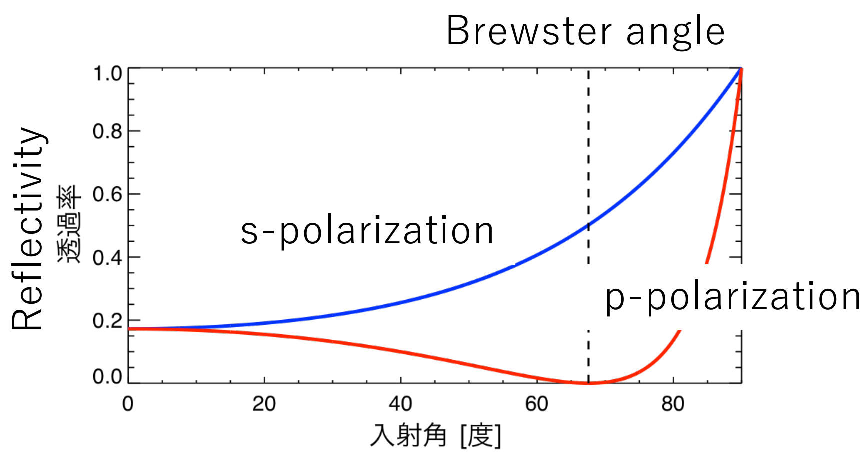

For p-polarization, zero-reflection (Brewster) angle appears.

Reflectivity for strong field : Si thin film (50nm)

s- and p-polarizations

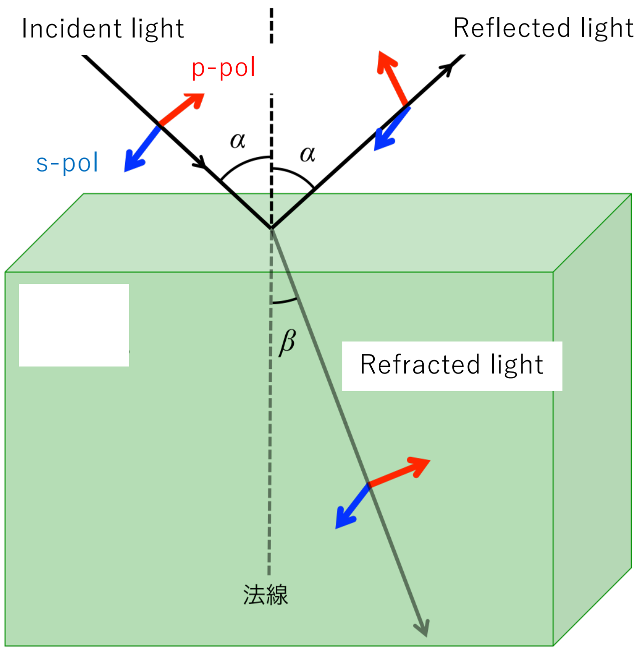

Brewster's angle appears robustly against intensity

Reflectivity

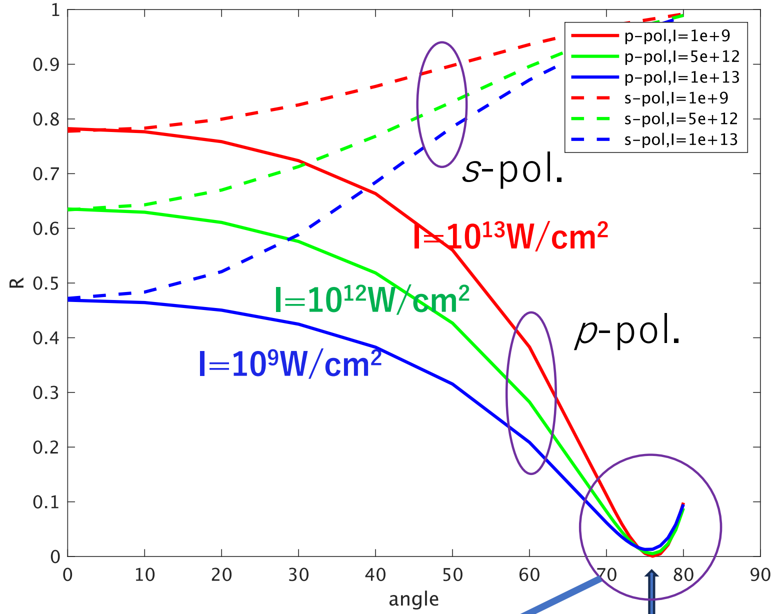

Brewster's angle

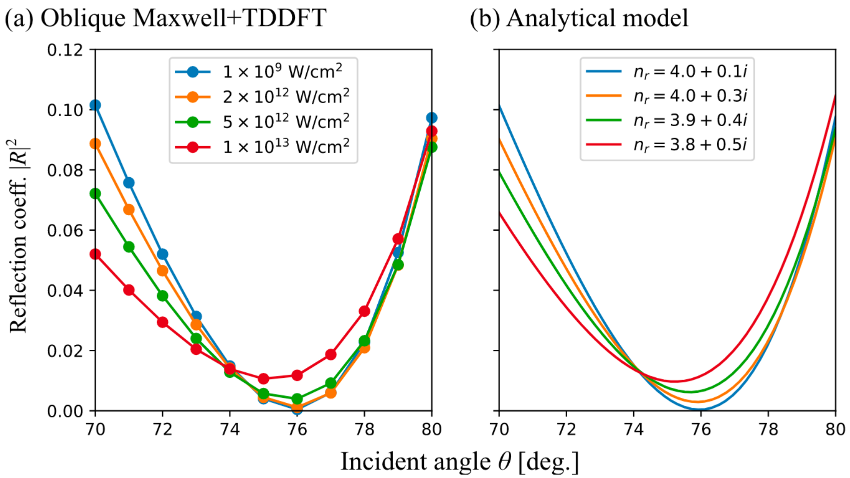

Nonlinearity described by the change of index of refraction

Surface Plasmon Polariton in linear electromagnetism

SPP exists at the M-R interface when evanescent field appears in R region.

Incident pulse couples when the momentum matching is satisfied.

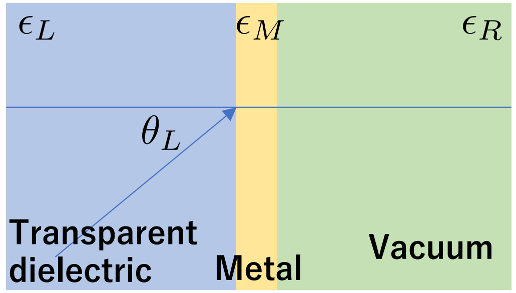

$$R = \left| \frac{A^r}{A^i} \right|^2$$

$$\frac{A^r}{A_i} = -\frac{r_{12} - r_{23} e^{2ik_M d}}{1 - r_{12} r_{23} e^{2ik_M d}}$$

$$r_{12} = \frac{f_{L,-}}{f_{L,+}}, \qquad r_{23} = \frac{f_{R,-}}{f_{R,+}} \qquad k_M = \frac{\omega}{c}\sqrt{\epsilon_M - n_L^2 \sin^2\theta_L}$$

$$f_{(R,L),\pm} = n_{(R,L)} \left\{ \frac{\sqrt{\epsilon_{(R,L)} - \epsilon_L \sin^2\theta_L}}{\epsilon_{(R,L)}} \pm \frac{\sqrt{\epsilon_M - \epsilon_L \sin^2\theta_L}}{\epsilon_M} \right\}$$

$$\sqrt{\epsilon_R - \epsilon_L \sin^2\theta_L} \to i\sqrt{\epsilon_L \sin^2\theta_L - \epsilon_R}$$

$\epsilon_L = 2.3,\ \epsilon_R = 1.0,\ \epsilon_M = -18.23 + 0.482i,\ d = 1000 \text{ au} = 52.9\ \text{Å}.$

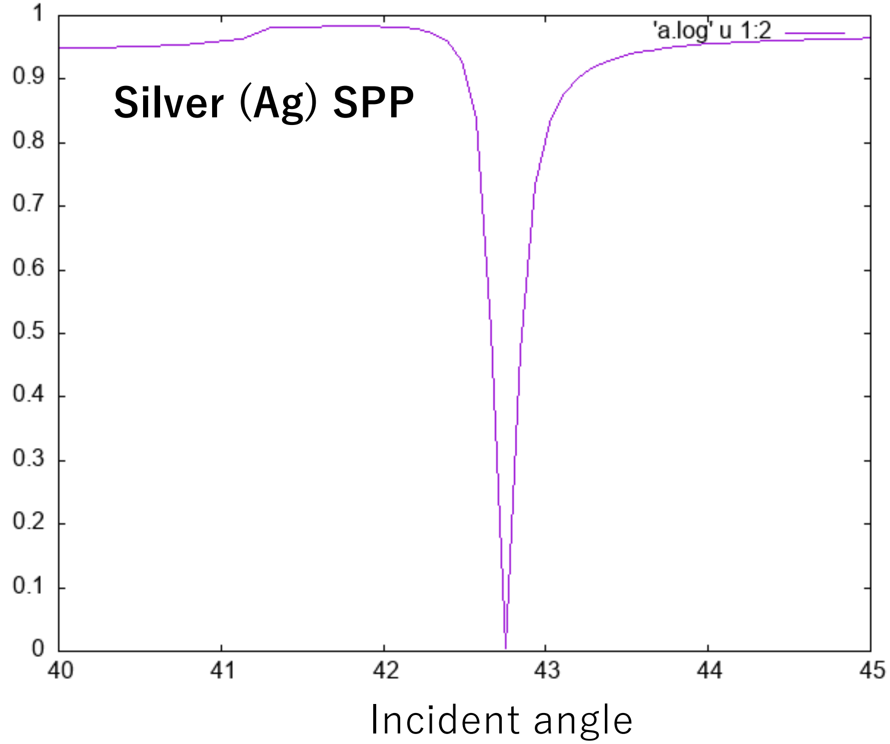

Surface Plasmon Polariton : Aluminum thin film (10nm)

Multiscale Maxwell-TDDFT calculation at oblique incidence

Kretchmann geometry

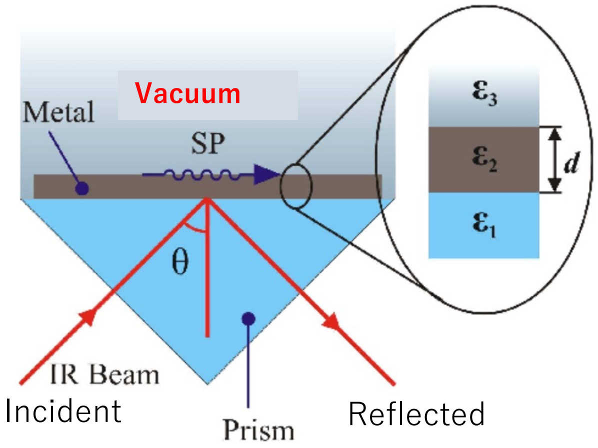

Surface plasmon mode appears when evanescent field appears in the vacuum region.

Weak pulse: $I=10^9$ W/cm^2, hw=1.5eV, 42 deg., *p*-polarization

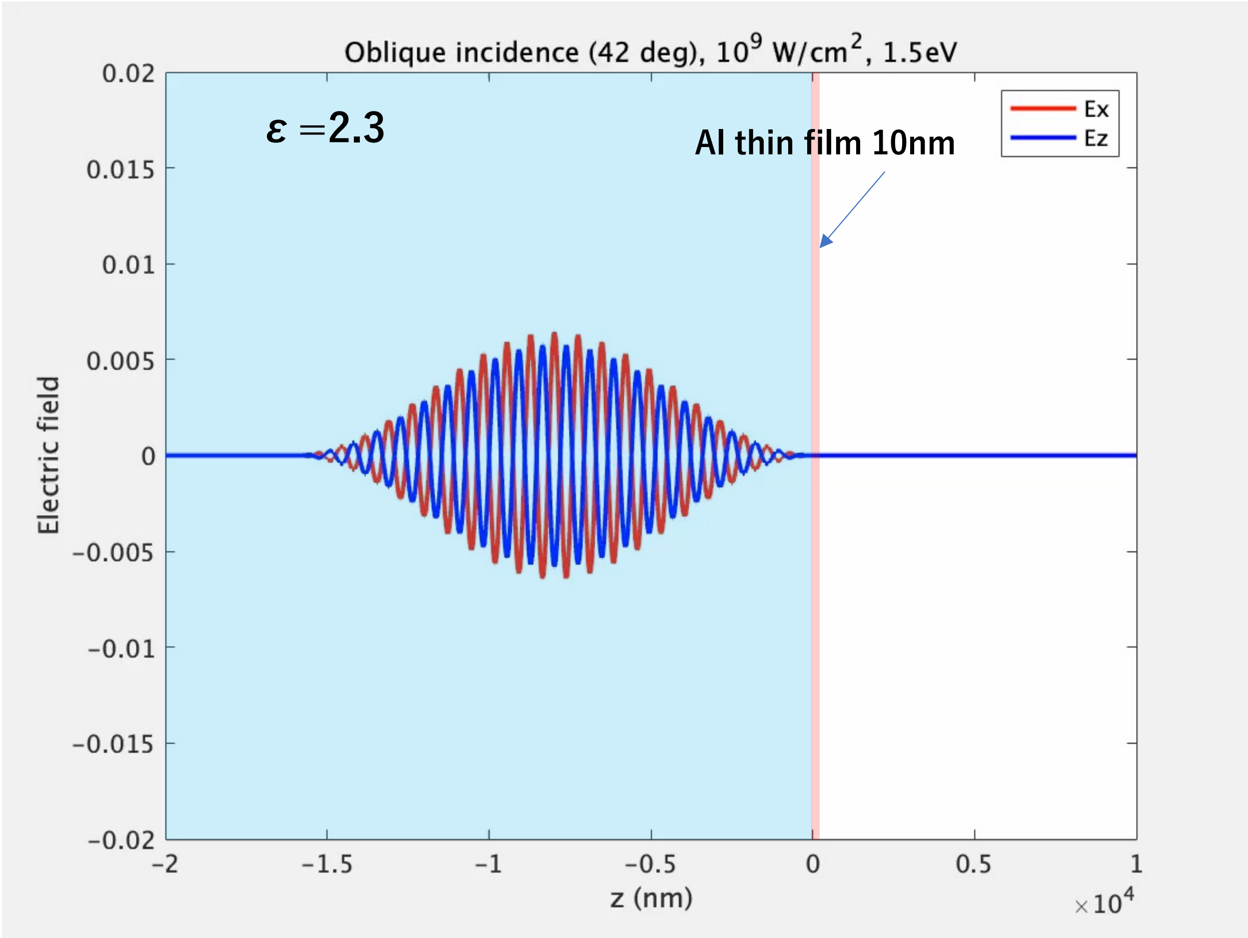

Multiscale Maxwell-TDDFT calculation at oblique incidence

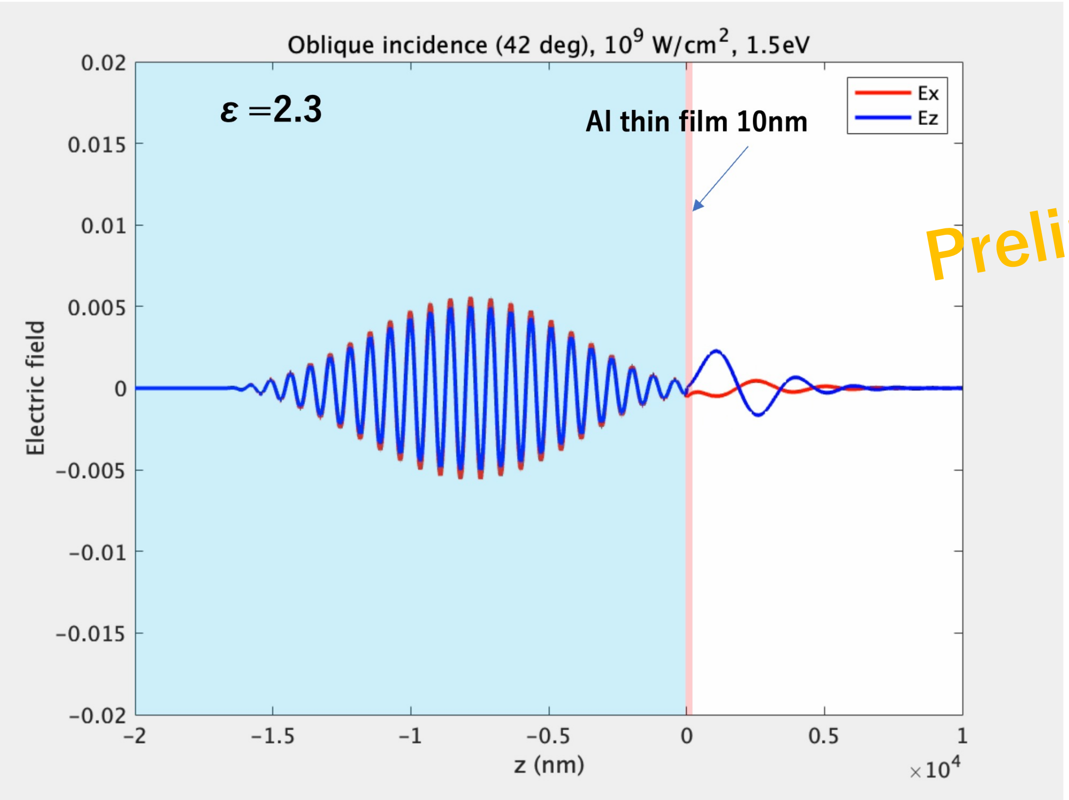

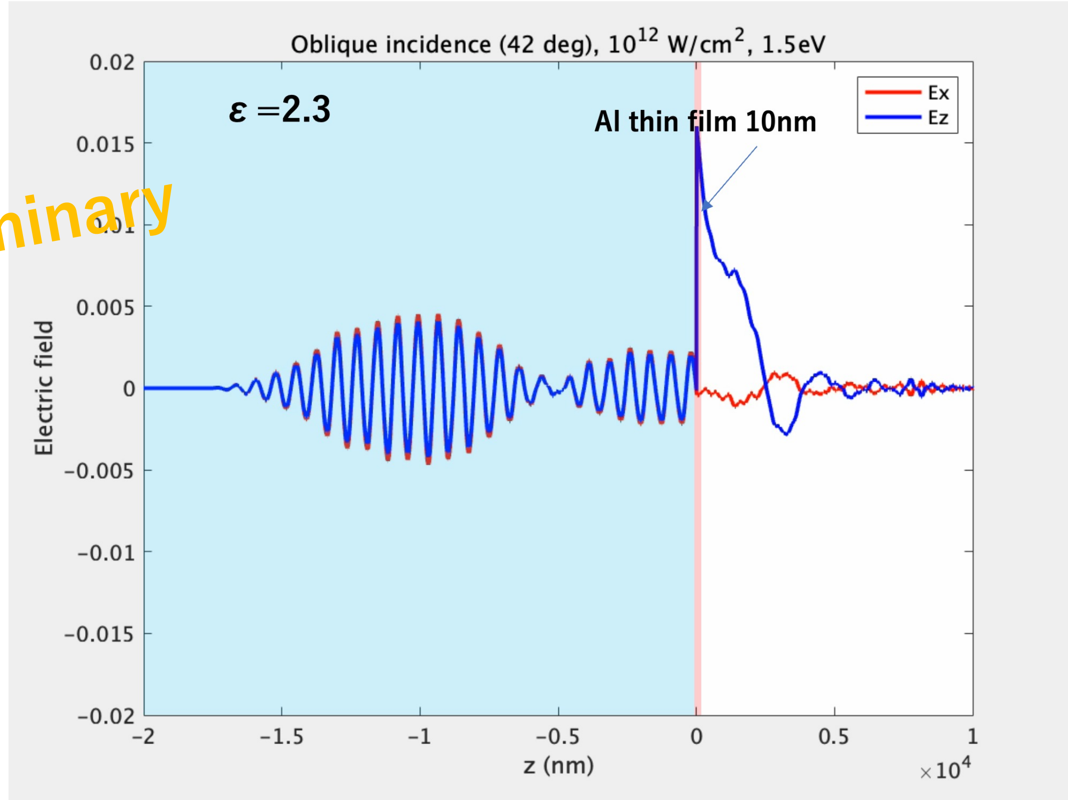

Strong nonlinearity! Only strong pulse shows coupling with surface plasmon.

Multiscale Maxwell-TDDFT calculation at oblique incidence

Kretchmann geometry

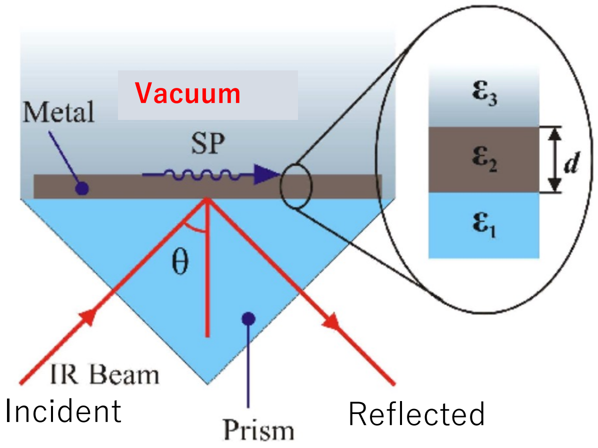

Surface plasmon mode appears when evanescent field appears in the vacuum region.

Angle dependence of reflectivity

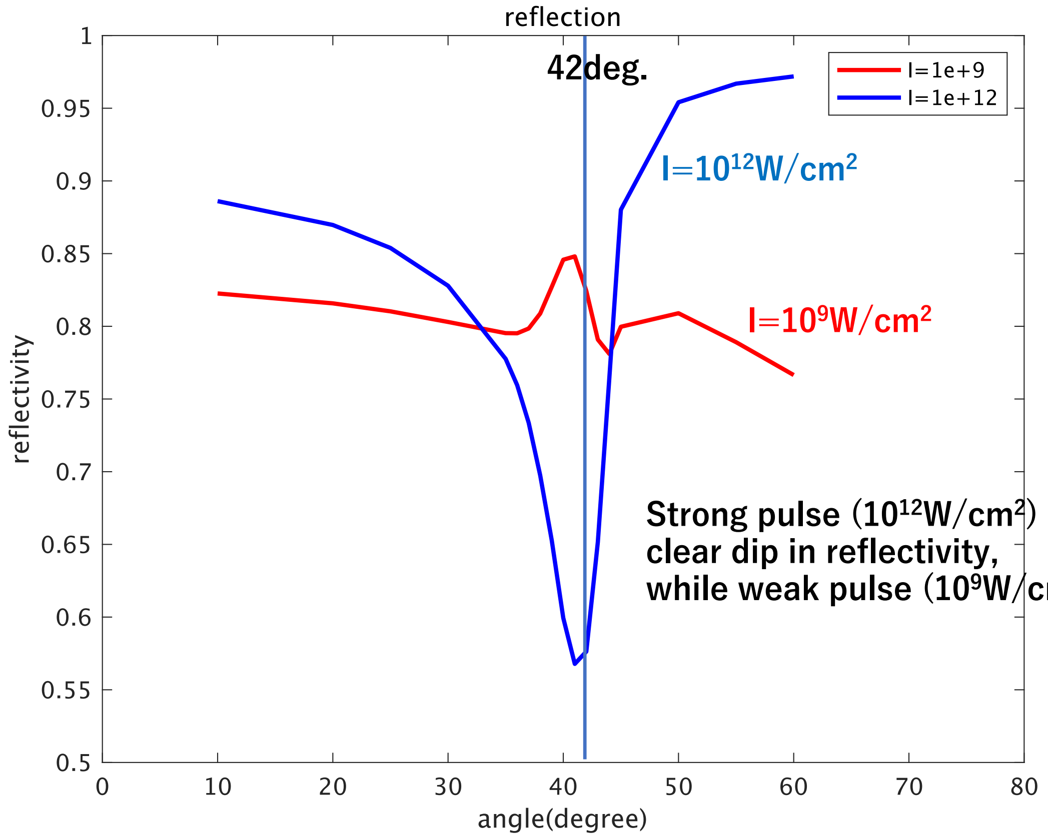

Strong pulse ($10^{12}W/cm^2$) shows clear dip in reflectivity, while weak pulse ($10^{9}W/cm^2$) does not.

Summary

In current frontier of optics characterized by ultrafast, nonlinear, and nonlocal, traditional EM or QM approaches are not sufficient.

We develop first-principles electromagnetic analysis, combining EM and QM (Real-time TDDFT)

There are two connection methods: macroscopic (multiscale) and microscopic (single-scale)

Applications include high harmonic generation, laser processing, plasmonic meta-surface etc.

All calculations use SALMON https://salmon-tddft.jp

Scalable Ab initio Light – Matter simulator for Optics and Nanoscience

Acknowledgement

Collaborators (SALMON project)

Atsushi Yamada
National Defence Academy Jpn.

Shunsuke Yamada
Kansai Photon Sci. Inst

Takashi Takeuchi
RIKEN

Arqum Hashmi
U. Tokyo

Mitsuharu Uemoto
Kobe Univ.

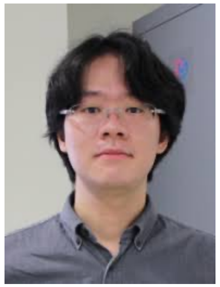

Yuta Hirokawa
Private Company

Shunsuke Sato
U. Tsukuba

Tomohito Otobe
Kansai Photon Sci. Inst.

Financial supports

CREST
戦略的創造研究推進事業
Core Research for Evolutionary Science and Technology

CDMSI

科研費
KAKENHI

Q-LEAP

Supercomputers

富岳

JCAHPC